CORROSION BEHAVIOUR OF ALUMINIUM–GRAPHENE NANO PLATELETS (AL/GNP) NANOCOMPOSITE

SUBASHINY A/P PRABAKARAN

FACULTY OF ENGINEERING
UNIVERSITY OF MALAYA
KUALA LUMPUR

2018

CORROSION BEHAVIOUR OF ALUMINIUM–GRAPHENE NANO PLATELETS (AL/GNP) NANOCOMPOSITE

SUBASHINY A/P PRABAKARAN

RESEARCH PROJECT SUBMITTED IN PARTIAL FULFILMENT OF THE REQUIREMENTS FOR THE DEGREE OF MASTER OF MATERIALS ENGINEERING

FACULTY OF ENGINEERING
UNIVERSITY OF MALAYA
KUALA LUMPUR

2018

UNIVERSITY OF MALAYA

ORIGINAL LITERARY WORK DECLARATION

Name of Candidate: SUBASHINY PRABAKARAN

Matric No: KQJ 170009

Name of Degree: MASTERS OF MATERIALS ENGINEERING

Title of ~~Project Paper~~/Research Report/~~Dissertation~~/~~Thesis~~ ("this Work"):

CORROSION BEHAVIOUR OF ALUMINIUM–GRAPHENE NANO PLATELETS (AL/GNP) NANOCOMPOSITE

Field of Study: CORROSION STUDY

I do solemnly and sincerely declare that:

(1) I am the sole author/writer of this Work;
(2) This Work is original;
(3) Any use of any work in which copyright exists was done by way of fair dealing and for permitted purposes and any excerpt or extract from, or reference to or reproduction of any copyright work has been disclosed expressly and sufficiently and the title of the Work and its authorship have been acknowledged in this Work;
(4) I do not have any actual knowledge nor do I ought reasonably to know that the making of this work constitutes an infringement of any copyright work;
(5) I hereby assign all and every rights in the copyright to this Work to the University of Malaya ("UM"), who henceforth shall be owner of the copyright in this Work and that any reproduction or use in any form or by any means whatsoever is prohibited without the written consent of UM having been first had and obtained;
(6) I am fully aware that if in the course of making this Work I have infringed any copyright whether intentionally or otherwise, I may be subject to legal action or any other action as may be determined by UM.

Candidate's Signature Date:

Subscribed and solemnly declared before,

Witness's Signature Date:

Name:

Designation:

CORROSION BEHAVIOUR OF ALUMINIUM–GRAPHENE NANO PLATELETS (AL/GNP) NANOCOMPOSITE

ABSTRACT

This study was conducted to study the effect of adding graphene reinforcement to aluminium matrix, on the composite's corrosion behavior. Aluminium-graphene nanoplatelet composites (Al/GNP) of different aluminium and graphene nanoplatelets composition percentages were produced.

The corrosion behavior of Al-5%GNP, Al-10%GNP and Al-15%GNP composites was examined in solutions of three different corrosion molarity i.e. 1M, 3M and 5M of sodium chloride (NaCl) solutions, via Cyclic Potentiodynamic Polarization method. The electrochemical test was followed by scanning electron microscopy (SEM) and energy dispersive spectrometer (EDS) investigations, to compliment the test results.

The study revealed that the presence of graphene and its increasing amount in the metal matrix composite (MMC), increases corrosion rate while decreasing the polarization resistance of aluminium. SEM/EDS examination of the corroded test materials indicated that the graphene in the MMC encouraged aluminium to corrode more, due to galvanic corrosion phenomenon. This effect was seen to be increasing when amount of graphene added was also increased.

Keywords: Aluminum corrosion, aluminum-graphene composite, electrochemical measurements, SEM/EDS investigations, sodium chloride.

CIRI-CIRI PENGHAKISAN ALUMINIUM–GRAFENA NANO PLATELETS (AL/GNP) NANOKOMPOSIT

ABSTRAK

Satu siri komposit nanoplatelet aluminium-grafena (Al / GNP) yang berlainan peratusan komposisi, iaitu Al-5% GNP, Al-10% GNP dan Al-15% GNP telah direka.

Tingkah laku kakisan Al-5%GNP, Al-10% GNP dan Al-15% komposit GNP diteliti dalam larutan natrium klorida (NaCl) dengan molarity berbexa, 1M, 3M dan 5M, menggunakan ujian potentiodinamik kitaran polarisasi (CPP). Kajian ini juga disampingi dengan pemeriksaan mikroskop elektron (SEM) dan penyiasatan spektrometer penyebaran tenaga (EDS).

Pengukuran kakisan menunjukkan bahawa kehadiran GNP dan peningkatan kandungannya meningkatkan kadar kakisan dan mengurangkan ketahanan polarisasi Al. Siasatan SEM / EDS mendedahkan bahawa kehadiran grafena mengaktifkan kakisan aluminium kerana berlakunya kakisan galvanik dan kesan ini bertambah dengan peningkatan kandungan grafena.

Kata kunci: kakisan aluminium, komposit aluminium-grafena, pengukuran elektrokimia, penyiasatan SEM / EDS, natrium klorida.

ACKNOWLEDGEMENTS

My master's degree research project journey wouldn't have been a smooth ride without the constant guidance of my supervisor, advisors, and unwavering help from family and friends. I would like to express my deepest gratitude to my supervisor, Dr.Nazatul Liana Sukiman, for her excellent guidance. Not forgetting to thank are Dr Masoud Sarraf, Ms. Waheeda Rahman and my course mate, Ms. Shalini Devi Ramaiya of University Malaya for their great advice and support in this project. I would also like to convey my deepest gratitude to my family, Mr Prabakaran & Ms Santhi, and Mr Ganeshwaran, for their relentless support and encouragement with their best wishes. Lastly, my heartiest gratitude to every well-wisher for their persistent support and encouragement. It would have been a tough journey without their ideas and support throughout the process.

TABLE OF CONTENTS

LIST OF FIGURES

LIST OF TABLES

LIST OF SYMBOLS AND ABBREVIATIONS

For examples:

^{o}C	:	Celcius
2D	:	Two dimension
3D	:	Three dimension
Al	:	Aluminium
Al/GNP	:	Aluminium/Graphene Nanoplatelets
AMMC	:	Aluminium metal matrix composite
CNT	:	Carbon nanotube
Cl	:	Chloride
CPP	:	Cyclic potentiodynamic polarization
EDS	:	Energy-dispersive spectroscopy
GNP	:	Graphene Nanoplatelets
Na	:	Natrium (Sodium)
NaCl	:	Sodium Chloride
MMC	:	Metal matrix composite
PCA	:	Process control agent
Pa	:	Pascal
SEM	:	Scanning electron microscopy
SiC	:	Silicon Carbide

CHAPTER 1: INTRODUCTION

1.1 Background

This research project studies the corrosion inhibition behaviour of graphene nanoplatelets added metal matrix composite (MMC), especially aluminium metal matrix composite (AMMC). Pure aluminium (Al) and its alloys are considered to be some the most versatile engineering materials across a broad range of applications (Dasari B.L., 2018). Aluminium is one of the most prevalently used element in many aspects of our life, being a key component of various applications. This is largely attributed to its highly desirable properties and ability to be applied in an endless range of applications.

Generally, pure aluminium is not suitable to be used as a heavy duty material for large structures, but it possesses excellent wet-corrosion resistance, compared to many other typically used metals, that is attributed to the highly protective oxide film barrier formed on the surface of metal almost immediately in a wide variety of environments.

Considering its lesser properties in its raw and pure nature, aluminium is often used as various alloy types. Typically, aluminium forms alloys with metals or non-metals such as manganese, magnesium, copper, silicon, tin and zinc. Aluminium alloys typically possess better product properties than pure aluminium material. Even then, there is a constant need to develop materials with better properties in all aspects, in this fast-developing global arena.

Aluminium has comparatively excellent mechanical properties and this has made it the second most widely used metal in the world today after steel. Alam et.al. have reported that it has a low density (2.7g/cc), superior malleability, good thermal conductivity (237W/mK), very low electrical resistivity (2.65x10-8 Ω m) and good formability. Its Young modulus is 70G Pa and its Vickers hardness is 160–350 MPa. Aluminium has a melting point of 660.32 °C and at high temperatures, its strength decreases (Alam S.N.,

2016). On top of this, aluminium also possesses good machinability, corrosion resistance, and a unique combination of other properties.

Just like metal alloys, metal matrix composites (MMC) are another type of metal/non-metal combination material. In order to widen the application of various metals in plenty more fields with better material properties, MMC have been studied and actively researched for past quarter of century. They have significant contributions to various important fields such as electronic, automotive and aerospace industries. This huge advancement is the result of continuous progress in developing various types of processing techniques and due to the ability to correlate the relationship between how composite structures are formed and their mechanical and electrochemical behaviour etc.

There is an increasing demand to produce aluminium and its alloy types with increased strength. Thus, in comes the composites as an alternative promising material with added material properties to solve the shortcomings of pure and alloys and keep up with the increasing demand for better material selections. To produce enhanced composite metal materials, there are various strengthening strategies and approaches proposed. One of them is the addition of strengthening secondary materials such as graphene and carbon nanotubes with the primary metallic materials. This approach has been gaining popularity over the years for providing significant improvements to various aspects of the metal composites such as mechanical and electrochemical properties by the addition of a small percentage of a strengthening material to the base metal material.

One such material type is carbon fillers. Researchers have long studied its variants, the carbon nanotubes (CNTs) and carbon fibers which act as strong reinforcements, having possessing promising Young's modulus. Unfortunately, these types of carbon fillers come at high cost, making it as one of the reasons carbon fillers are less preferred in the competitive market when mass production of composite material has to be considered.

This prompted and still prompts the discovery of much cheaper but a better material for mass composite productions.

Graphene was first discovered in 2004. Despite a pretty late discovery, it has received widespread attention, thanks to its amazing electrical and mechanical properties and its applicability in various products and fields, from energy harvesting and nanoelectronics to drug delivery in medical applications. This has made graphene an excellent candidate for further research in various applications, as a good choice of advanced material. Graphene is a two-dimensional one-atom-thick sheet of carbon in the form of hexagonal lattice, and it is the basic structural unit of graphite (Katsnelson, 2007).

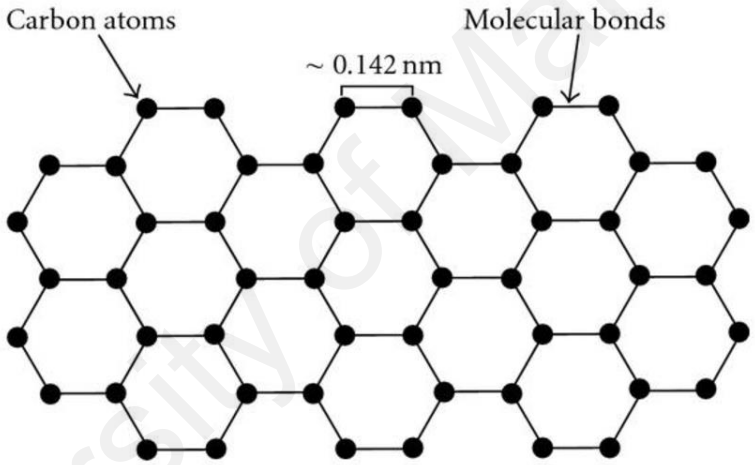

Figure 1.1: Schematic of the structure of a graphene sheet (Katsnelson, 2007)

Graphite is essentially made up of hundreds of thousands of layers of graphene. This renders graphene more unique properties than graphite. For a long time, graphite has been a common reinforcement used for steel structures. But as a structural material of its own, graphite is not generally utilized since it has sheer planes. Despite this flaw, graphite is still one of the strongest material discovered, being 40 times stronger than diamond and 300 times more than A36 structural steel.

Just like the structure of graphene, graphene nanoplatelets are essentially stacked layers of graphene. It has a thickness of up to approximately 100nm thick (Liu J., 2013). Frank I.W. et.al. reported that GNP 2 to 8nm thick have a Young's modulus

approximately 0.5Tpa (Frank I.W., 2007), which is higher than aluminium's 70Gpa. Hence, studies have been conducted to identify if aluminium metal's strength and toughness can be enhanced by reinforcing the matrix using GNP (Nieto A., 2017). Indeed, aluminium's various natural material properties can be enhanced by introducing a reinforcement such as GNP to overcome the monolithic aluminium material's limitations. It can improve aluminium's natural stiffness, strength and toughness.

There have been studies which have used GNP as a coating to reinforce the metal interface and these studies show improved corrosion resistance (Zhou F, 2013). However, it is not entirely known if the same can be achieved by dispersing the GNP, instead, in the matrix itself. This can be done by fabricating Al/GNP composite using powder metallurgy technique.

In order to explore GNPs as potential reinforcements for corrosion resistant applications, powder metallurgy technique was used to produce Al/GNP composite. When these composites are subjected to electrochemical tests, polarization curves for their corrosion behaviour were obtained and validated by analysing the corrosion deposits formed on the composite matrices under SEM microscopy.

Corrosion is the deterioration of a material, usually a metal or an alloy, which results from a reaction with its environment. An example of a corrosion behavior is the rusting of steel when immersed in seawater. To complete a corrosion process and anode, a cathode, an electrolyte and an electrical path connecting them, are required. When these elements are present in the right environment, corrosion is a natural and inevitable process which, however, can be controlled with the right measures. If left uncontrolled, corrosion is capable of progressing and damaging the material, with irreversible effects also. Essentially corrosion is induced when there is a chemical and thermodynamic imbalance between the metal and its environment.

In nature, only certain precious metals such as platinum, gold and silver and non-precious metal such as copper are found in their metallic state. Apart from these, other types of commonly used metals are generally processed from their oxides or mineral ores. These metals, regardless of their status, are chemically and thermodynamically unstable and revert back to their more stable compound forms, given the opportunity. In order to protect their raw form from corrosion attack, some metals tend to form a protective barrier on the surface, which can prevent or slow down their corrosion depending on the environment of the sample (Shaw B.A., 2006).

Corrosion occurs in many different form. Each of these forms is affected by the material specification, nature of the corrosive environment and length of exposure to determine the form of corrosion. Some of the most common forms of corrosions are general or uniform corrosion, galvanic corrosion, pitting corrosion, stress corrosion cracking, crevice corrosion, corrosion fatigue, and so on (CHAPTER 4 - TYPES OF CORROSION: Materials and Environments, 2006). The economic impact of corrosion has been huge. According to the World Corrosion Organization, the annual cost of corrosion in 2010 was US $2.2 trillion, which is more than 3% of the world's gross domestic product (GDP; US $63.0 trillion) (Mondal, 2016). Therefore, there is increased demand for robust techniques and materials that inhibit corrosion and lengthen the life cycle of products made of metal alloys, to insure great environmental and economic savings.

There are several techniques reported in the literature (Zheng SX, 2010) to preserve metals from corrosion, including surface passivation followed by painting and/or varnishing, as well as galvanic and sprayed coatings. These methods may have several imperfections such as low corrosion and mechanical resistance of passivated surfaces, low wear ability of paints, and pores and other defects in spray coatings. An alternative

solution for preserving the metallic components is to produce composite metallic materials with materials which exhibit corrosion-inhibiting properties, such as graphene.

The studies revealed that prepared graphene and graphene oxide based hybrid and especially composite coatings well inhibit corrosion of the metals. This definitely increases the lifetime and stability of the metal parts and equipment made from these materials, helping to preserve materials and energy, thus helping to develop a more sustainable society.

1.2 Problem Statement

Corrosion poses a big threat to the integrity and durability of pure, alloyed or composite metal based components. For example, NaCl-induced corrosive environments are one of the most commonly found and their effect on metal composites are not widely studied yet. To overcome the setbacks posed by corrosion, there are plenty of anti-corrosion protecting techniques available with their own pros and cons. Considering that graphene nanoplatelets addition in metals to produce nanocomposites is widely getting more attention, more studies is required to study their anti-corrosion behaviour in corrosive environments before implementing in wide scale applications. So, this research project aims to investigate the effect of NaCl-induced corrosive environments of different concentrations for aluminium–graphene nanoplatelets (Al/GNP) nanocomposites.

1.3 Research Aim and Objective

The main aim of this study was to investigate the corrosion behaviour of composite formed by graphene, a non-metal, addition to pure aluminium metal. However, the extent of the corrosion resistant property of the MMC needs more study, to identify how and if graphene particles will induce corrosion of different degree. So, the objectives to achieve through this research was

i) To investigate the corrosion behavior of aluminium graphene nanocomposites with different graphene percentage composition in sodium chloride solution

ii) To study the corrosion morphology of Al graphene nanocomposite with different graphene percentage composition

1.4 Scope of Studies

Graphene has long been generally thought to be a perfect membrane that can block completely the penetration of impurities and molecules (Tsetseris, 2014). However, it's efficacy in providing adequate corrosion protection for a metal matrix composite has largely been understudied.

The scope of this research is to investigate and understand corrosion behavior of aluminium when reinforced with graphene with different percentage. This investigation covers whether graphene of higher percentage protects the composite from corrosion defects or induce added corrosion attack, when dispersed in the metal matrix. Besides, the MMC's pittig corrosion tendency with increasing graphene presence, was also observed and evaluated over the course of this study. SEM and EDS were used to study the corroded surface of aluminium MMCs.

CHAPTER 2: LITERATURE REVIEW

This chapter focuses in depth on aluminium and graphene nanoplatelets and on the corrosion behaviour of graphene-reinforced aluminium matrix nanocomposites as reported in past studies. This literature review helps to justify the novelty of this research topic.

Aluminium naturally has high intrinsic corrosion inhibition properties. It is gifted by nature to naturally form an oxide layer on its air-exposed surface, which protects the metal surface and matrix from further oxidation (Ahmad Z., 2011). But, this isn't sufficient to completely fool proof aluminium protection against corrosion, since the surface of this oxide layer is composed of numerous defects. These defects sometimes can get overpowered by some harsh natural elements and the metal surface gets exposed to the raw elements. It is to be noted that such defects actually make easy way for an otherwise insulated (oxidised) metal surface to be electrically conducting (Ahmad Z., 2011). In such situation, the environment is conducive to form pitting corrosion on the aluminium metal's surface and naturally these surface defects act as primary sits for pits to form. Thus, these potential pit sites which result from local breakdown of the oxide film, also add on the localised corrosion of aluminium surface. All of these contribute to the detailed fundamental and practical scrutiny aluminium, including the various types it can be found as, and their corrosion behaviour receive over the years (Thompson, 1996).

Further to that, another thing to be noted is the barrier film formed by aluminium's exposure to natural environment is chemically reactive when coming in contact with aqueous solution of different pH values. Through this process the oxide layer formed on the surface would start thinning in low or high pH valued solutions while it starts to gather significant hydration at solutions having intermediate pH values (Sahu S.C., 2013).

2.1 An Insight into Aluminium Metal

One of the most abundant elements on earth is aluminium, being the third most abundant, and comprising about 8% of Earth's crust mass. It is the most abundant structural metal. However, in real, aluminium is only found in stable combination with other materials, prominently in the form of silicates and oxides. Its presence was identified by Sir Humphrey Davy, who first addressed it as "aluminium". Post this, countless years of painstaking research had passed before it could be extracted as a material of its own from the base ore and even more years to go before it could be prepared in commercially-viable state for plenty of economical applications. A scientist named Wöhler, then, successfully calculated the density of aluminium, providing further evidence for this material's lightweight and malleability properties (Richards, 1887).

Aluminium is one of the most lightweight metals available today, making it a favourite in various fields. However, pure aluminium has very limited applications, so it is often made into various types of alloys by combining with other metals with superior qualities. Aluminium and its alloys' properties depend mainly on their intrinsic values developed during their manufacturing processes. Their chemical composition and microstructural features undergo complex interaction when the metal is subjected to various processes such as solidification, thermal treatment and, for wrought alloys, deformation processing (Richards, 1887).

Aluminium and its alloys properties form several unique combination of properties, by natural, or by their manufacturing processes, making it one of the most sought after construction material. These properties are dependent mainly on the purity of the base aluminium metal. Aluminium's low density (2.7 g/cm3) makes it highly favourable and has better corrosion resistance properties compared to other similar valued metals, along

with possessing high mechanical strength influenced by the proper alloying and heat treatments (Davis, 1999).

Apart from these three basic properties, there are several others which make aluminium a highly sought-after material in various field applications. They can be categorised as physical properties and chemical properties.

2.1.1 Aluminium: physical, mechanical and chemical properties

Aluminium has a silver-metal shade colour and is found at an atomic number13 and atomic weight of 26.9815 g/mol. Aluminium has a face-centred cubic crystal structure which stays intact up until the melting temperature, as seen in Figure 2.1 below.

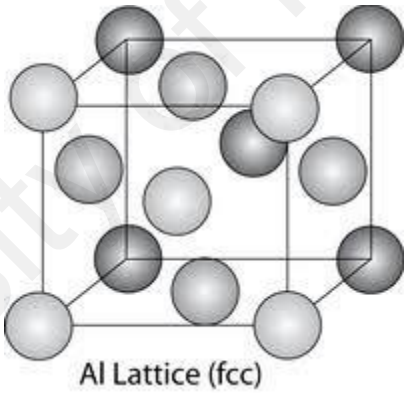

Figure 2.1: Al FCC crystal structure

In this crystal structure, the atoms are packed at a close distance of 2.863Å at room temperature (Richards, 1887) and the metal's stacking fault is at 200 mJ/m2. Aluminium is one of the lightest metals, which in turn give it the advantageous strength by alloying. It is an excellent conductor of heat and electricity, light reflector and corrosion resistor. Apart from that, aluminium is also one of the non-magnetic variants of metals plus being non-toxic. It can be fabricated by all known metal working processes. However, these properties can be manipulated through alloying, cold-working and heat treating methods.

Tensile strength of pure aluminium is 90MPa. This can be modified and strengthened up to 700Mpa, for some heat-treatable alloy variants.

Aluminium alloys can get as strong as structural steel when fabricated into the right alloy and extruded properly. For example, Aluminium alloy 7000 series can be manipulated to reach strength levels up to 07 to 0.8 GPa when processed properly. But, this alone doesn't make them on par with structural steel. Even with increased strength, they still have considerably limited fracture toughness and strain localisation of environmentally-sensitive cracking.

Furthermore, aluminium's Young's modulus (E = 70,000 MPa) is only one third that of steel, which in turn is advantageous for aluminium. Under the same static and dynamic loading circumstances, aluminium behaves more elastically, whereby the metal is able to go back to its original shape and size. Naturally, aluminium is very malleable. It can be easily shaped into a variety of shapes (Richards, 1887).

Aluminium's excellent malleability, is favourable for its extruding process. It can be bent and formed in both hot and cold conditions. We can form any kind of complex shapes by extruding aluminium pieces, without having to mechanically joining them. And as a matter of good fact, this results in better final product which is less likely to defect over time. In certain shape and form, aluminium possesses better properties than some other metals or materials. Table 2.1 below shows some important physical properties; however, these properties are affected by the purity of aluminium.

Table 2.1: Properties of Aluminium (Richards, 1887)

Property	**Value**
Atomic Number	13
Atomic Weight (g/mol)	26.98152
Valency	3

Crystal Lattice	Face centred cubic
Boiling point (^oC)	2480
Melting point (^oC)	660.2
Electrical Resistivity at 20^oC (μ.cm)	2.69
Thermal conductivity (o-100oC) (cal/cms. OC)	0.57
Mean specific heat (0-100OC) (cal/g^oC)	0.219
Coefficient of Linear Expansion (0-100^oC) (x10^{-6}/^oC)	23.5
Density (g/cm^3)	2.6898
Electrical Resistivity at 20^oC (μΩcm)	2.69
Modulus of Elasticity (GPa)	70
Poisson Ratio	0.34

2.2 Graphene and Its Properties

2.2.1 Graphene: the forerunner of the 2D material family

Graphene is a one-atom-thick layer of sp2-bonded carbon atoms. It has a honeycomb crystal lattice and the atoms are densely packed together (Kumar P., 2014). This unique two dimensional material was first established in 2004 Prof. Andre Geim and Kostya Novoselov via mechanical cleavage of highly oriented pyrolytic graphite (HOPG), for which they were awarded the Nobel Prize in Physics (Lee, 2012).

On a topological point of view, graphene can be regarded as the basic unit of various types of carbon materials (Geim, 2007), such as zero-dimensioned buckyballs, one-dimensioned nanotubes and three-dimensioned graphite, as shown in Figure 2.2 below.

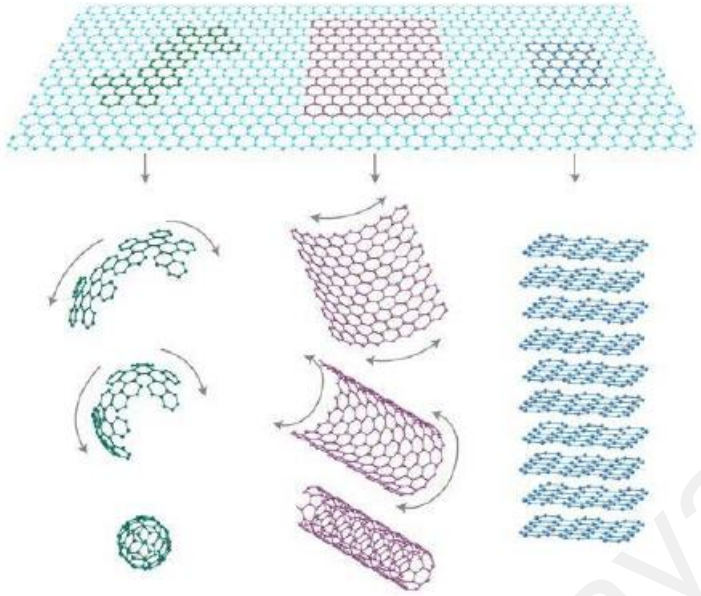

Figure 2.2: Schematic illustration on how other carbon allotropes can be formed by graphene (Geim, 2007)

2.2.2 Graphene and electronic properties

Graphene is very well-known for its remarkable electronic, mechanical, optical and chemical properties. It is an excellent electronic conductor. Its valence and conduction band crossover at six discrete Dirac points of the Brillouin zone, though which a zero band gap semiconductor can be produced.

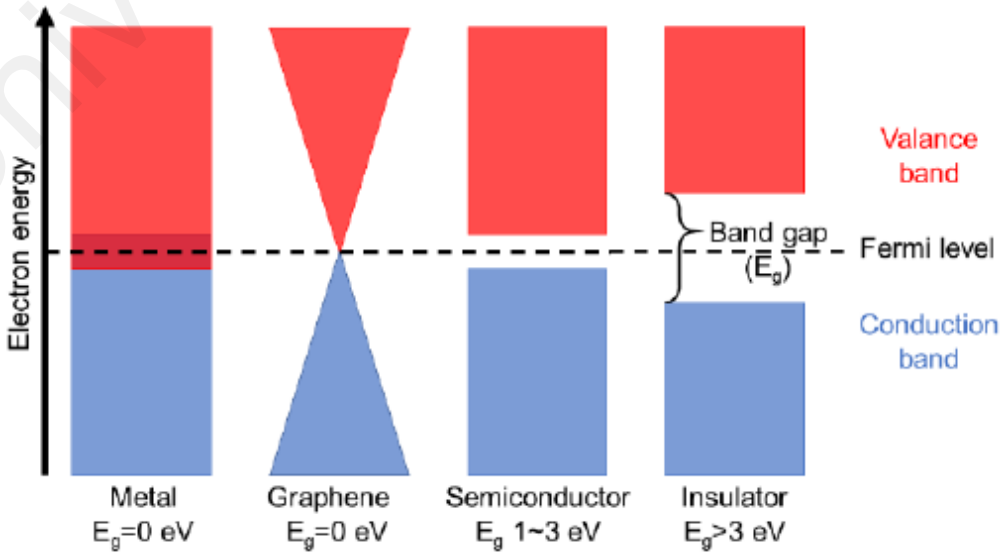

Figure 2.3: Band structures of metal, graphene, semiconductor and insulator

It has been noted that graphene's charge carriers behave as "massless relativistic particles" (Dirac fermions) (Potts J.R., 2011). Graphene exhibits anomalous integer quantum Hall effect and high electron mobility at room temperature (>200,000 cm2/V). Furthermore, there are numerous other remarkable electronic characteristics for graphene. Moreover, ballistic transport of charge carriers is available at micron-scale at room temperature. Graphene has a resistivity value which can get as low as $1\times10-8\ \Omega\cdot m$, which is even lower than that of Ag ($1.59\times10-8\ \Omega\cdot m$), Cu (1.68 x 10-8 Ω·m), Au (2.44 x 10-8 Ω·m) and Al (2.82 x 10-8 Ω·m), testifying graphene as a better conductor than these metals. Although the unique electronic properties of graphene make it promising in application of electronic devices, they are generally not beneficial when it comes to application in anticorrosive coatings. This is because galvanic corrosion is introduced when the noble and highly conductive graphene layer is in direct contact with the metal s (Geim, 2007).

2.2.3 Graphene and thermal properties

Thermal conductivity of graphene experiments were initially conducted on a suspended single-layer graphene, which has a value of $5300\ W\cdot m-1\cdot K-1.47$. The value of thermal conductivity of graphene is higher than those reported for carbon nanotubes (CNTs) ($3000\ W\cdot m-1\cdot K-1$ for multi wall CNT40 and $3500\ W\cdot m-1\cdot K-1$ for single wall CNT. Later studies propose the initial results on graphene's ultrahigh thermal conductivity to be overestimated, however, a range between $1500–2500\ W\cdot m-1\cdot K-1$ was still obtained (Balandin, 2008), indicating that graphene is an excellent thermal conductor. Graphene's superior thermal conductivity makes it an outstanding material for thermal management applications, such as condensation heat transfer system and heat spreaders.

2.2.4 Graphene and optical properties

Single layer graphene is reported to have an opacity of 2.3% and negligible reflectance (<0.1%) to incident white light (Nair, 2008), as presented in Figure 2.4. The absorption of light increases linearly with the number of graphene layers, which is 2.3% for each additional graphene layer. Due to interference effects that strongly enhance the optical contrast, graphene supported on Si/SiO_2 can be imaged with the contrast scaling linearly with the number of graphene layers. Besides, graphene's combined electrical and optical properties pave the way for its application in photonics and optoelectronics, such as transparent conductors, infrared photodetectors, light emitting devices, touch screens, solar cells and THz devices etc. (Nair, 2008).

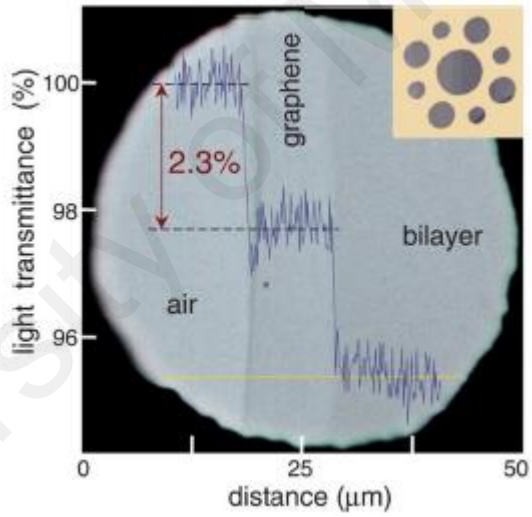

Figure 2.4: First measurement on graphene's opacity (Nair, 2008)

2.2.5 Graphene and mechanical properties

Graphene is the strongest known material, up to 200 times stronger than steel of the same weight (Shinohara, 2015). Measurements on the mechanical properties of monolayer graphene was initially carried out with an atomic force microscope (AFM), (Lee, 2008). In this study, the intrinsic tensile strength of graphene was found to be 130 GPa while the Young's modulus was measured to be 1 TPa and has a failure strain up to

12% (Lee, 2008). Not just these properties, studies have been conducted to measure tensile and compressive strain in graphene, as well, using Raman spectroscopy. These studies monitored the change of G and 2D peaks of the material under stress, and their results showed that graphene can sustain tensile strains over 1.3%, whereas in compression the maximum load is 0.7%. Moreover, defects in graphene have been proved to lower the mechanical strength of pristine graphene (Zandiatashbar, 2014).

Furthermore, the remarkable mechanical properties of graphene have been exploited to reinforce polymer matrix. For instance, it is reported that when graphene nanoplatelets are loaded with a fraction of 0.1% in a polymer matrix, the overall mechanical properties of the composite structure, in terms of Young's modulus and tensile strength, are greatly enhanced with respect to the starting polymer matrix (Rafiee, 2009).

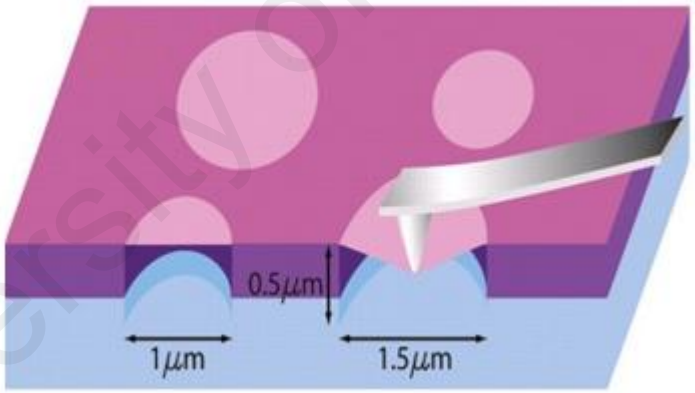

Figure 2.5: Schematic illustration on the nano-indentation experiment for initial measurement of graphene's mechanical properties. (Lee, 2008)

2.2.6 Graphene and permeability properties

Graphene has been experimentally demonstrated to be impermeable to all gases including helium (Bunch, 2008). Furthermore, a perfect single layer graphene is also impermeable to hydrogen atoms at ambient conditions, due to the high energy barrier for tunneling through graphene's dense electronic cloud (Miao, 2013). However, it has been

experimentally proved that defect-free pristine graphene is instead highly permeable to thermal protons at ambient conditions (Achtyl, 2015). For AB-stacked bilayer graphene, where carbon atoms are centered on the hexagonal rings of the next layer, protons are, however, not able to penetrate through (Achtyl, 2015). Moreover, protons can also be transported through graphene in aqueous solution through atomic defects via the Grotthuss mechanism (Achtyl, 2015).

2.2.7 Graphene and other properties

Theoretical specific surface area of graphene has been found to be considerably large (2630 m^2/g) (Stoller, 2008), as well as having high aspect ratio (i.e., the ratio of lateral size to thickness). The wettability and surface free energy of graphene is reported by Wang, S et al. (Wang, 2009). From their results, graphene is hydrophobic with a water contact angle of 127°, which is higher than that of graphite (98.3°). The surface energy of graphene in dry nitrogen, which implies the interaction strength between graphene and nitrogen, is reported to be about 115 mJ/m^2 (van Engers, 2017). Moreover, experimentally measured results for the adhesion energy of chemical vapour deposited graphene on Cu and Ni are 12.8 and 72.7 $J \cdot m^{-2}$, respectively (Das, 2013).

2.2.8 Graphene nanoplatelets

Graphene nanoplatelets (GNP) form the smallest size graphene unit molecules can be purchased commercially. They are available in sizes 6-8 nm thickness and possess a bulk density of 0.03 to 0.1 g/cc. Oxygen content in GNP is less than one percentage only while the majority (99.5 wt%) is carbon and the residual acid content is also 0.5 wt%. They are found as black granules (Kumar P., 2014).

Figure 2.6: Graphene nanoplatelets aggregate (Kumar P., 2014)

Just as the bigger sized graphene sheets, graphene nanoplatelets are excellent heat and electricity conductors. However, GNPs provide lower thermal contact resistance at lower loading levels. This essentially results in it having higher thermal conductivity, compared to other variants of carbon particles such as nanotubes or carbon fibers, due to the platelet morphology. GNPs are capable of reducing the thermal expansion coefficient of various polymer variants while increasing the ultimate use temperature values. Besides, GNPs can offer increased stability of the dimension structure of material it is used with, along with the operating temperature range. Moreover, GNPs are also capable of further reducing permeability or diffusion coefficients of the matrix material it is used for reinforcements, compared to plain graphene sheets. Asmatulu et.al (2015) reports that permeability is significantly influenced by the particle size of the additive, and in general, larger diameter particles provide greater reductions in permeability (Asmatulu R., 2015).

Compared to multi-walled carbon nanotubes (MWCN), GNPs are advantageous in that they have higher specific surface area. Furthermore, they are also less prone to twisting thus diffuse/disperse easier into the matrix and improve the mechanical properties. GNP is also much easier and cheaper to be worked with, with reduced health hazards, compared to other variants of carbon particles. These multifunctional property enhancements

provided by GNPs make them a much favoured additions as reinforcement to various matrices in a variety of applications such as semiconductor industry (Kumar P., 2014).

2.3 Corrosion and Its Effects

2.3.1 Impact of corrosion globally

Corrosion is generally described as chemical or electrochemical reactions of metals or alloys with the environment, reactions which undesirably deteriorate the properties of the materials in a way that may lead to failure to perform their function (J. Liu, 2015). Degradation and failure of metals due to corrosion not only lead to direct economic loss (e.g. loss of metals and leakage of oil or gas) but also indirect catastrophic disasters (e.g. breakdown of bridges and leakage of nuclear power plants), as shown in Figure 2.1. According to reported studies, (H. Alhumade, 2016) (M. Mo, 2016) (J. Mondal, 2016) cost of corrosion can be up to 5% of Gross Domestic Product (GDP) in USA, UK, and China.

2.3.2 Principles of Corrosion

There are generally two types of corrosion, including “dry” corrosion and “wet” corrosion (J. Liu, 2015). “Dry” corrosion is normally used for metal-gas or metal-vapor reactions, where oxidation of metals and reduction of non-metals take place at the same area. This form of corrosion (M. Mo, 2016) is more commonly termed as “oxidation” of metals as direct chemical reactions between metals and environment are normally involved. On the other hand, in the case of “wet” corrosion, oxidation (or dissolution) of metals (anodic reaction) and reduction of non-metals (cathodic reaction) can occur at different places with corresponding electron transfer processes to complete electrochemical reactions. In this research project, the term “corrosion” refers to “wet” corrosion unless otherwise specified.

As corrosion is essentially a chemical reaction process, its thermodynamics follows the Second Law of Thermodynamics (A. Ahmadi, 2016). For a corrosion process, the change in Gibbs free energy must be negative to allow the reactions to spontaneously take place. Besides, as corrosion includes electron transfer processes, Faraday's Law can be applied to express Gibbs free energy.

Therefore, the overall potential ($E_{cathode}$ - E_{anode}) for electrochemical reactions should be positive in a corrosion process. Values of potential in electrochemistry are normally referred to standard hydrogen electrode (SHE). This is defined with a potential value of 0 V and forms the basis for scaling of potential for other redox half reactions. When the reduction potential of a metal is more negative, it is more likely to serve as an anode to be oxidized and allow cathodic reaction to be coupled and initiate corrosion process. For example, an anode of Fe (-0.44 V) can be corroded in water with a corresponding cathodic oxygen reduction process (0.40 V). As the potentials listed in Table 2.2 are potential values at standard conditions (e.g. 25 °C, 1 atm, 1 mol/L for aqueous species), these standard potential values need to be transformed to actual potential values using the Nernst equation.

Table 2.2: Standard reduction potentials at 25 °C for common half-reactions

Half-Reaction	$\mathscr{E}°$ (V)	Half-Reaction	$\mathscr{E}°$ (V)
$F_2 + 2e^- \rightarrow 2F^-$	2.87	$O_2 + 2H_2O + 4e^- \rightarrow 4OH^-$	0.40
$Ag^{2+} + e^- \rightarrow Ag^+$	1.99	$Cu^{2+} + 2e^- \rightarrow Cu$	0.34
$Co^{3+} + e^- \rightarrow Co^{2+}$	1.82	$Hg_2Cl_2 + 2e^- \rightarrow 2Hg + 2Cl^-$	0.27
$H_2O_2 + 2H^- + 2e^- \rightarrow 2H_2O$	1.78	$AgCl + e^- \rightarrow Ag + Cl^-$	0.22
$Ce^{4+} + e^- \rightarrow Ce^{3+}$	1.70	$SO_4^{2-} + 4H^+ + 2e^- \rightarrow H_2SO_3 + H_2O$	0.20
$PbO_2 + 4H^+ + SO_4^{2-} + 2e^- \rightarrow PbSO_4 + 2H_2O$	1.69	$Cu^{2+} + e^- \rightarrow Cu^+$	0.16
$MnO_4^- + 4H^+ + 3e^- \rightarrow MnO_2 + 2H_2O$	1.68	$2H^+ + 2e^- \rightarrow H_2$	0.00
$2e^- + 2H^+ + IO_4^- \rightarrow IO_3^- + H_2O$	1.60	$Fe^{3+} + 3e^- \rightarrow Fe$	−0.036
$MnO_4^- + 8H^+ + 5e^- \rightarrow Mn^{2+} + 4H_2O$	1.51	$Pb^{2+} + 2e^- \rightarrow Pb$	−0.13
$Au^{3+} + 3e^- \rightarrow Au$	1.50	$Sn^{2+} + 2e^- \rightarrow Sn$	−0.14
$PbO_2 + 4H^+ + 2e^- \rightarrow Pb^{2+} + 2H_2O$	1.46	$Ni^{2+} + 2e^- \rightarrow Ni$	−0.23
$Cl_2 + 2e^- \rightarrow 2Cl^-$	1.36	$PbSO_4 + 2e^- \rightarrow Pb + SO_4^{2-}$	−0.35
$Cr_2O_7^{2-} + 14H^+ + 6e^- \rightarrow 2Cr^{3+} + 7H_2O$	1.33	$Cd^{2+} + 2e^- \rightarrow Cd$	−0.40
$O_2 + 4H^+ + 4e^- \rightarrow 2H_2O$	1.23	$Fe^{2+} + 2e^- \rightarrow Fe$	−0.44
$MnO_2 + 4H^+ + 2e^- \rightarrow Mn^{2+} + 2H_2O$	1.21	$Cr^{3+} + e^- \rightarrow Cr^{2+}$	−0.50
$IO_3^- + 6H^+ + 5e^- \rightarrow \frac{1}{2}I_2 + 3H_2O$	1.20	$Cr^{3+} + 3e^- \rightarrow Cr$	−0.73
$Br_2 + 2e^- \rightarrow 2Br^-$	1.09	$Zn^{2+} + 2e^- \rightarrow Zn$	−0.76
$VO_2^+ + 2H^+ + e^- \rightarrow VO^{2+} + H_2O$	1.00	$2H_2O + 2e^- \rightarrow H_2 + 2OH^-$	−0.83
$AuCl_4^- + 3e^- \rightarrow Au + 4Cl^-$	0.99	$Mn^{2+} + 2e^- \rightarrow Mn$	−1.18
$NO_3^- + 4H^+ + 3e^- \rightarrow NO + 2H_2O$	0.96	$Al^{3+} + 3e^- \rightarrow Al$	−1.66
$ClO_2 + e^- \rightarrow ClO_2^-$	0.954	$H_2 + 2e^- \rightarrow 2H^-$	−2.23
$2Hg^{2+} + 2e^- \rightarrow Hg_2^{2+}$	0.91	$Mg^{2+} + 2e^- \rightarrow Mg$	−2.37
$Ag^+ + e^- \rightarrow Ag$	0.80	$La^{3+} + 3e^- \rightarrow La$	−2.37
$Hg_2^{2+} + 2e^- \rightarrow 2Hg$	0.80	$Na^+ + e^- \rightarrow Na$	−2.71
$Fe^{3+} + e^- \rightarrow Fe^{2+}$	0.77	$Ca^{2+} + 2e^- \rightarrow Ca$	−2.76
$O_2 + 2H^+ + 2e^- \rightarrow H_2O_2$	0.68	$Ba^{2+} + 2e^- \rightarrow Ba$	−2.90
$MnO_4^- + e^- \rightarrow MnO_4^{2-}$	0.56	$K^+ + e^- \rightarrow K$	−2.92
$I_2 + 2e^- \rightarrow 2I^-$	0.54	$Li^+ + e^- \rightarrow Li$	−3.05
$Cu^+ + e^- \rightarrow Cu$	0.52		

2.3.3 Types of corrosion

Corrosion can be categorised into a few variants based on the corrosion-induced effects. They are uniform corrosion, intergranular corrosion, galvanic corrosion, localized corrosion, dealloying, stress corrosion cracking and so on (J. Liu, 2015). However, in this research project, the focus is to discuss the first three types of corrosion. Uniform corrosion is the most common type of corrosion, and is named as such as the entire exposed surface of metals is under attack. Uniform corrosion attack contributes to majority of metal destruction. However, it is often considered relatively better than other types in terms of safety because it is predictable, preventable and manageable.

Localized corrosion, on the other hand, attacks specific areas of metals and includes pitting (e.g. cavities on surfaces), crevice (e.g. gaps between two joining surfaces) and filiform (e.g. under painted surfaces) corrosion. Localized corrosion is more insidious

than uniform corrosion, because it is generally faster, harder to prevent and causes more serious damage to metals.

Galvanic corrosion or "bimetallic corrosion", is defined by NACE International (E.M. Fayyad, 2016) as "corrosion associated with the current resulting from an electrical coupling of dissimilar electrodes in an electrolyte". This type of corrosion is dangerous, in that it accelerates any existing corrosion process and can be mostly prevented by a proper corrosion design. Figure 8 presents the galvanic corrosion of iron coupling with tin, which is more noble than iron hence less susceptible to corrosion. When iron is oxidized, Fe^{2+} ions from the electrolyte react with oxygen in the water to form iron hydroxides or iron oxides and precipitate on the surface as rust. Electrons from iron are transferred from iron to tin, driven by the difference in individual corrosion potential between the two metals. The tin surface can act as a large cathode and greatly increases the rate of cathodic oxygen reduction reaction, which spontaneously accelerates the corrosion rate of iron (J. Liu, 2015) (A.B. Ikhe, 2016).

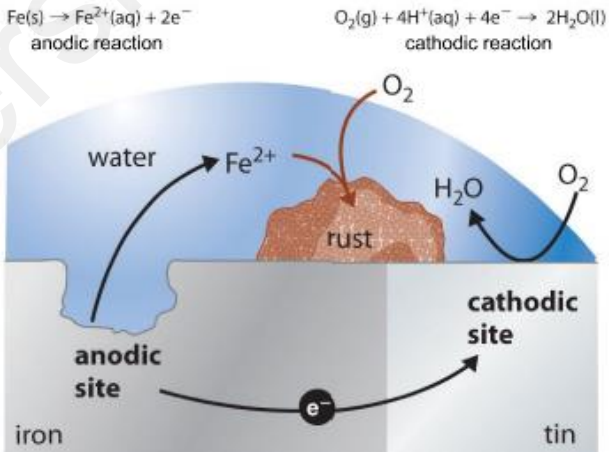

Figure 2.7: Schematic illustration of galvanic corrosion of iron coupled with tin. (A. Ahmadi, 2016)

2.3.4 Corrosion protection

Metals and alloys are important structural materials for various industries, it is therefore of vital importance that these materials are protected from corrosion not only to increase the lifetime of industrial systems and decrease economic loss, but also to reduce its adverse impact on the environment and society (e.g. pollution or explosion). So far, many different types of corrosion protection strategies have been developed (Ahmad Z., 2011) including surface pretreatment, anticorrosive coatings, cathodic protection, anodic protection, use of corrosion inhibitors and corrosion-resistant materials (Aneja K.S, 2017) (Rashad M, 2017). According to a recent study on cost of corrosion (J. Mondal, 2016), expenditures on coatings, corrosion resistant materials and surface treatments dominates the direct cost of corrosion in China, as presented in Figure 2.8, indicating that these strategies are currently of great importance in corrosion protection.

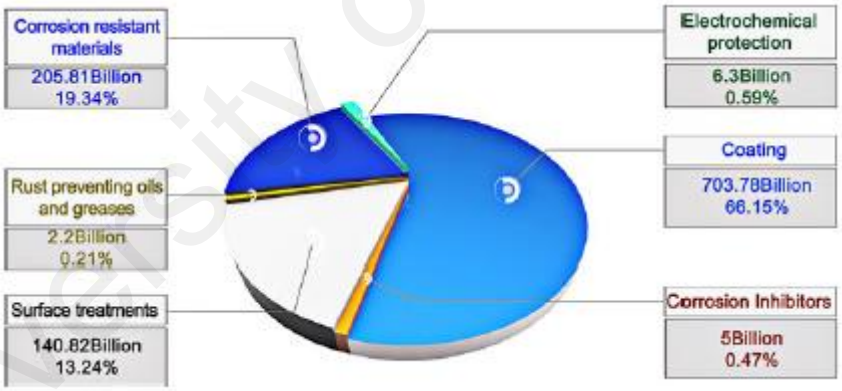

Figure 2.8: The direct costs of corrosion (RMB) in China in 2014 by protection strategies (J. Mondal, 2016)

Surface treatment is applied to change the state, chemical composition and/or microstructure of metal surfaces so as to make it more stable (e.g. plasma ablation, chemical etching (J. Liu, 2015).On the other hand, Corrosion-resistant materials, such as stainless steels and titanium alloys, are used in various applications (e.g. deep-sea and

aerospace equipment) to provide sufficient corrosion resistance in specific working conditions (J. Mondal, 2016).

2.4 Aluminium-Graphene Composite and Its Properties

2.4.1 Overview of metal-matrix composites

A metal-matrix composite (MMC) is a composition of at least two material constituents. In this combo, at least one material is a metal while the other could be any other kind of material or organic compound such as ceramic. MMC can be easily identified among other type of materials due to their unique characteristics of reinforcement used during fabrication. They include particles, whiskers or short/continuous fibers (Z. Hu, 2016). These different types of reinforcements act to increase the strength, thermal capabilities and stiffness of the primary material. They also help to decrease thermal expansion coefficient of the final MMC material. However, not every material combination can result in enhanced properties. There can be some unexpected chemical reactions taking place between the matrix and reinforcements. Not just that, thermal stresses due to thermal expansion mismatch between the reinforcements and the matrix should be taken into account.

Metal-matrix composites have established many applications in various industries, over the years. This is largely attributed to the fact that these materials' specifications can be designed accordingly. They are well-known to have a wide range of structural and thermal management applications. MMCs have higher-temperature operating limits than the basic primary and secondary constituent parts, individually. It is possible to tailor-design these MMC's according to custom specifications to have enhanced thermal conductivity, stiffness, strength and other properties (Alam. S.N., 2016).

Compared to monolithic materials, MMC have better fatigue and wear resistance and lower coefficients of thermal expansion. These advantages are why they are becoming more popular in electronics and thermal management applications (Alam. S.N., 2016).

2.4.2 Aluminium-Matrix Composites

Among various matrix materials available on the market, aluminium is widely used in the fabrication of the MMCs. Low weight, ease and prevalence of processing techniques, low cost, high thermal and electrical conductivity – all these characteristics make it a good candidate for versatile applications. The most commonly used materials as a reinforcement in the aluminium-matrix composite are usually graphite (C), carbon fibers (CF), silicon carbide (SiC) and alumina (Al_2O_3) while main manufacturing methods used to produce aluminium MMCs are squeeze casting, infiltration and powder metallurgy.

The main problem encountered when manufacturing the aluminium-matrix composites are the interfacial chemical reactions possible to occur in high temperatures as well as lack of wettability between the reinforcement and the matrix. Several solutions can be considered to mitigate the risk of aforementioned reactions such as making changes to the compositions of the matrix, applying reinforcement coatings and control of process parameters. Reinforcing the metal matrix by a secondary reinforcement material through modification of matrix composition has received wide attention over years. Rashad et al. have utilized the semi powder metallurgical technique and successfully produced aluminium matrix composite reinforced with graphene nanoplatelets (GNP) (Rashad M P. F., 2014). Bartolucci et.al reported that these graphene particles purportedly act as fillers in the aluminium matrix to further enhance the metal's intrinsic properties (Bartolucci S.F., 2011).

2.4.3 Aluminium-Graphene Composites

Aluminium/graphene nanoplatelets composite is the main subject of this research project. There are different types of graphene-reinforced MMCs reported in literature, among them graphene-reinforced aluminium matrix composite is the first. Bartolucci et al. successfully managed to fabricate Al/GNP MMC composite using powdered aluminium metal and graphene nanoplatelets using ball milling, hot isostatic pressing and extrusion methods (Bartolucci S.F., 2011). This Al/GNP variant, however, had reduced hardness and strength values compared to pure aluminium and MMC formed by reinforcing aluminium using multi-walled carbon nanotube (CNT). This inferiority is due to the formation of aluminium carbide during the fabrication process through consolidation and heating and extrusion process.

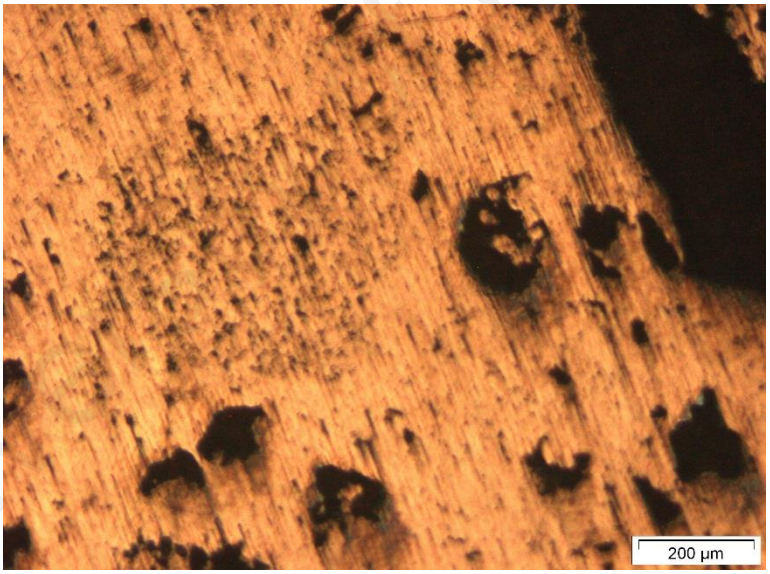

Figure 2.9: Optical micrographs of Al–0.05 wt-% graphene composites

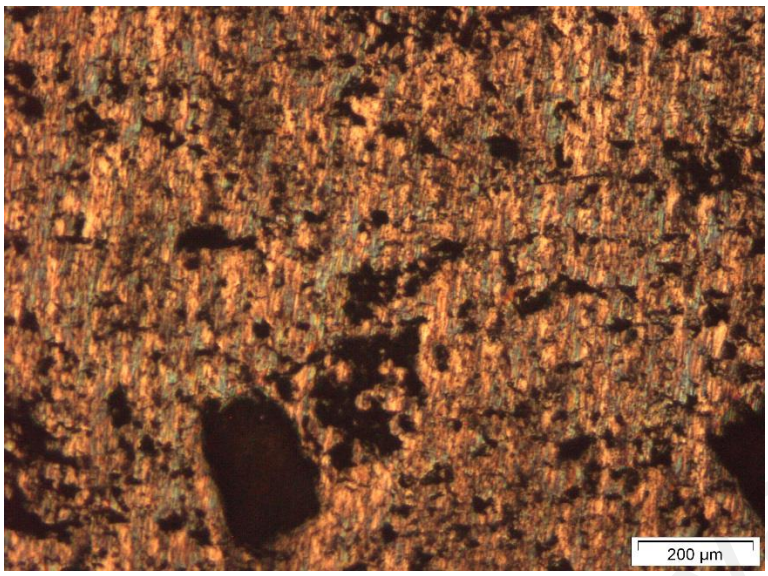

Figure 2.10: Optical micrographs of Al–0.1 wt-% graphene composites

Figure 2.9 and 2.10 illustrate the optical micrographs of graphene composites. Following that, another team studied aluminium reinforced with GNPs by flake powder metallurgy method and then compacted and extruded (J. Wang, 2012). In this experiment, the Al/GNP composites reinforced with 0.3 wt% of GNP had tensile strength which was a 62% more than the normal aluminium metal. This study proved for the first time that GNPs are actually effective method of reinforcement in an MMC, though not tested with other types of metals.

Deriving from the characteristics of aluminium and graphene, a composite of these two materials seems to be of high potential in thermal management applications due to characteristics which should be possible to obtain: high thermal conductivity, tailorable thermal expansion coefficient and low density. However, there are some main problem issues regarding Al/GNP composites' fabrication. Temperature 660.32°C is the melting point of aluminium and above this there are chemical reaction occurring between graphene and aluminium. As a result of aforementioned reactions, aluminium carbide (Al_4C_3) particles would be created (Etter, 2007). This phase is usually formed on the interphase border and deteriorates properties like thermal conductivity and strength. In

order to avoid such reactions the manufacture process of Al/GNP should be carefully performed in "safety" temperatures. The most popular methods to produce Al/GNP composite are liquid infiltration and powder metallurgy. During liquid infiltration process Al_4C_3 phase may be easily created when melted aluminium infiltrates the graphene preform for some time. The amount of time when graphene stays in contact with melted aluminium decides if the reaction occurs. The risk of aluminium carbide creation increases with time and temperature. In order to mitigate this risk, coating of the reinforcement is usually preferred over dispersing it in the metal matrix. The manufacturing method of such composites which allows controlling parameters like temperature and time is the powder metallurgy. Therefore, for the purpose of performed research, powder metallurgy has been chosen to manufacture the aluminium graphene used in this.

2.4.4 Aluminium-Graphene Composite and Corrosion

When a material is chosen for a particular purpose, its corrosion behavior in different types of environments must be well-considered, among other things. Corrosion is one of the major causes for failure for materials susceptible to its effects. MMCs and their corrosion behavior are largely influenced by the matrix composition, matrix microstructure, methods used to fabricate the composite and even the filler material's size and distribution on the matrix (Sherif E.M., 2011). As such, choosing the correct reinforcement for the matrix is extremely important as it has great influence on the corrosion resistance properties. This applies to the case of aluminium-based composites as well, since naturally aluminium can form a protective oxide barrier which provides its own corrosion resistance. Therefore, by adding these reinforcement particles, the continuity of this barrier formation on the metal's surface is hindered and this leads to more sites on the MMC's surface which is prone to corrosion attack.

Studies have shown that adding graphene nanoplatelets in material matrices has improved the MMC's corrosion resistance (Asmatulu R., 2015) (Kirkland N.T., 2012) (Misˇkovic´-Stankovic V., 2014). Especially in the study conducted by Misˇkovic´-Stankovic V. et.al., the E_{ocp} values of the graphene coated copper was found to be around 20 mV more positive than bare copper. Furthermore, the test materials' PDS measurements also registered a drop in current density, while graphene was still found on the material surface even after 40 days exposure via EIS measurement (Misˇkovic´-Stankovic V., 2014). It is to be noted that in this study, graphene was introduced in the form of coating on the metal. Based on these studies, it was learnt that graphene influenced the corrosion process induced in the investigated metal kinds in more than one way. In the experiment using nickel tablets, graphene primarily slowed the anodic dissolution reactions for nickel while for another study using copper, the metal was undergoing cathodic reduction reactions (Kirkland N.T., 2012).

So, it has been shown in past experiments that coating metals with graphene and polymer/graphene composites improves the corrosion resistance behavior of these metals. However, will this yield the same result when graphene is dispersed in the metal's matrix itself, is another question yet to be explored widely, especially with aluminium with its vast application previously discussed. It could enhance corrosion-resistant behavior or worsen it and studying this is very crucial, indeed. Due to its promising mechanical properties, Al/GNP composites of plenty of variations have been fabricated and tested for their strength and durability. The same hasn't been done to evaluate these variants' corrosion behavior and if yes, are numbered. Furthermore, these studies are mostly performed in only one type of corrosive aqueous environment, i.e. 0.1M NaCl solution. Studies on the corrosion behavior of Al/GNP MMC with different GNP composition in corrosive solutions of different severity also hasn't been studied yet to identify if the degree of alkalinity/acidity will influence the corrosion inhibition properties of an

Al/GNP composite where the protective GNP is present is different amounts. So, it isn't known how increasing degree of a corrosive environment's concentration would affect the corrosion inhibition properties of graphene embedded in metal matrix. This research project aims to study corrosion behavior of an aluminium composite reinforced with GNP in such variables.

CHAPTER 3: METHODOLOGY

3.1 Materials Preparation

3.1.1 Preparation of Al/GNP Samples

Aluminium of 99% purity and graphene nanoplatelets (GNP) were used to fabricate the Al/GNP composite with different compositions.

1) Aluminium powder was obtained commercially. This aluminium powder was ball milled to achieve refined and homogenized microstructure. The process was done in an argon gas filled stainless steel chamber and the metal was agitated using different stainless steel milling balls at different rotational speeds. In addition, stearic acid and methanol were added to the milling, to be used as process control agents (PCA). They are used to prevent powders from sticking to the balls and the jar wall. The ball to powder ratio of 10:1 enabled it to achieve a fine powder microstructure and minimize cold welding of the aluminium particles.
2) GNPs were cleaned in an ultasonicator using acetone for one hour. While this is being done, simultaneously, the ball-milled fine aluminium powder was also mechanically agitated in an acetone solution.
3) Following ultrasonification, the aluminium slurry formed in the acetone solution and the GNP particles were slowly added and mixed on a volume ratio of 95:5, using a mechanical agitator for an hour. This is to ensure a homegenous mixture is obtained.
4) Post this, the mixture was filtered and to remove the moisture in it, has been vacuum dried for 12 h at 70^{o}C to obtain the composite powder. This dry composite powder was pressed in a die at room temperature, under the pressure of 80-85 kN to obtain tablet with Ø1.95 x 0.3 cm (h) dimensions and 3g weight.

5) Process of compacting is followed by sintering. The tablets were sintered in inert, argon gas supplied, muffle furnace at 600^{o}C for 6h.

The same methods as above were used to fabricate Al/GNP composite with Al-10% GNP and Al-15% GNP composition.

Figure 3.1: Compacted and sintered final Al/GNP tablet (same for all three GNP compositions)

To use the samples in more solutions, each cylindrical tablet was cut into 6 equal pieces using wire cut method. The final test sample (Al-5%GNP) for each test looks as in Figure 13 below with a 5 cents coin size as the reference. Mirror-polished surface can be seen on the top. The result are the same for Al-10%GNP and Al-15%GNP, as well.

Figure 3.2: Size of final test sample (5 cents as size reference)

3.1.2 Preparation of NaCl (Aq) solutions

i. Preparation of 1M (4.0%) NaCl solutionl

1) 40g of NaCl pellet is weighed and added into a 500ml beaker.
2) 200ml distilled water is added to the above and stirred in a cold water bath till it is completely dissolved.
3) Then, this mixture is transferred into a 1000ml volumetric flask, filled up to the mark with distilled water and shaken well.

ii. Preparation of 3M (12.0%) NaCl solution:

1) 120g of NaCl pellet is weighed and added into a 500ml beaker.
2) 200ml distilled water is added to the above and stirred in a cold water bath till it is completely dissolved.
3) Then, this mixture is transferred into a 1000ml volumetric flask, filled up to the mark with distilled water and shaken well.

iii. Preparation of 5M (20.0%) NaCl solution:

1) 200g of NaOH pellet is weighed and added into a 500ml beaker.
2) 200ml distilled water is added to the above and stirred in a cold water bath till it is completely dissolved.
3) Then, this mixture is transferred into a 1000ml volumetric flask, filled up to the mark with distilled water and shaken well.

3.2 Experiment setup

3.2.1 Electrochemical Corrosion Test

- Preparation of Sample for Test

1) The 95 %, 90 % and 85 % Al containing Al/GNP samples were, first and foremost, grinded and polished to ensure the surface tested is free of impurities.
2) Using a SiC paper of 2400 grit, the working surface of the samples was grinded. Following that, the surface was polished to a mirror finish using a MicroPolish™

Alumina 0.3μm alumina slurry. Then, they were ultrasonicated for 2 minutes and dried in room temperature.

3) Post sample preparation, the samples' mirror polished surface images were captured using optical microscopy.

- Preparation of Electrochemical cell for Cyclic Potentiodynamic Polarization Test

1) A three-electrode electrochemical cell was built to run the CPP electrochemical tests.
2) Al/GNP composite sample, Al-5% GNP, was used as a working electrode.

In this three-cell electrochemical cell, saturated Calomel Electrode (Hg_2Cl_2) served as reference electrode while platinum mesh electrode served as the counter electrode. The non-polarizable potential of the working electrode is measured with respect to the Saturated Calomel Electrode. The reference electrode is connected electrically with the working electrode. On the other hand, the CPP voltmeter's negative terminal is connected to the working electrode and the positive to the reference electrode.

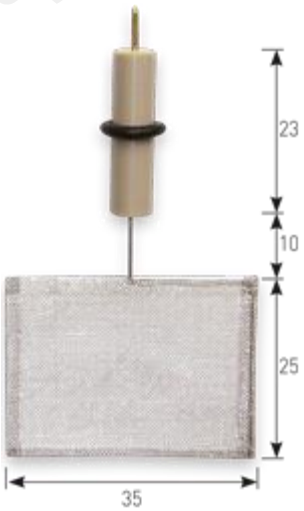

Figure 3.3: Platinum mesh electrode as counter electrode in CPP

- Conducting CPP Test

1) The Al/GNP sample for electrochemical measurements was prepared by enclosing the non-mirror finish side in aluminium foil and immersed in NaOH solution to be tested for a duration of 20h. The test coupons were not mounted, as they should have been ideally, prior to suspension in the solutions, due to certain circumstance. Instead, they were suspended using a piece of thread with the intention of having only the mirror-finished surface be in contact with the corrosive solution. The non-mirror finished surface of each test coupon was covered up using aluminium foil. Even then, some of the corrosive solution could have come in contact with the non-mirror finished surface over the course of experiment. Each Al/GNP sample with different GNP percentage were first immersed in NaCl solutions of different molarities for 20h prior to CPP testing. This was based on a similar experiment run by (Sherif E.M., 2011). In that study, all the electrochemical experiments were recorded after the working electrodes (MMC with graphite dispersed in the matrix) were immersed in the test solution for 40 min and 72 h before measurements. Thus, current study was also modeled based on this similar study, with the intention of conducting CPP test at 20h and at 72h gaps. This was so that weight loss of the test coupons could be studied. However, post the 20h immersion-CPP test, the idea to continue with 72h immersion-CPP test was dropped, since the weight loss was discovered to be too small and negligible. Due to unavailability of a fresh sample for each MMC with different GNP percentage, CPP test was proceeded using test coupons immersed for 20h in the NaCl solutions.

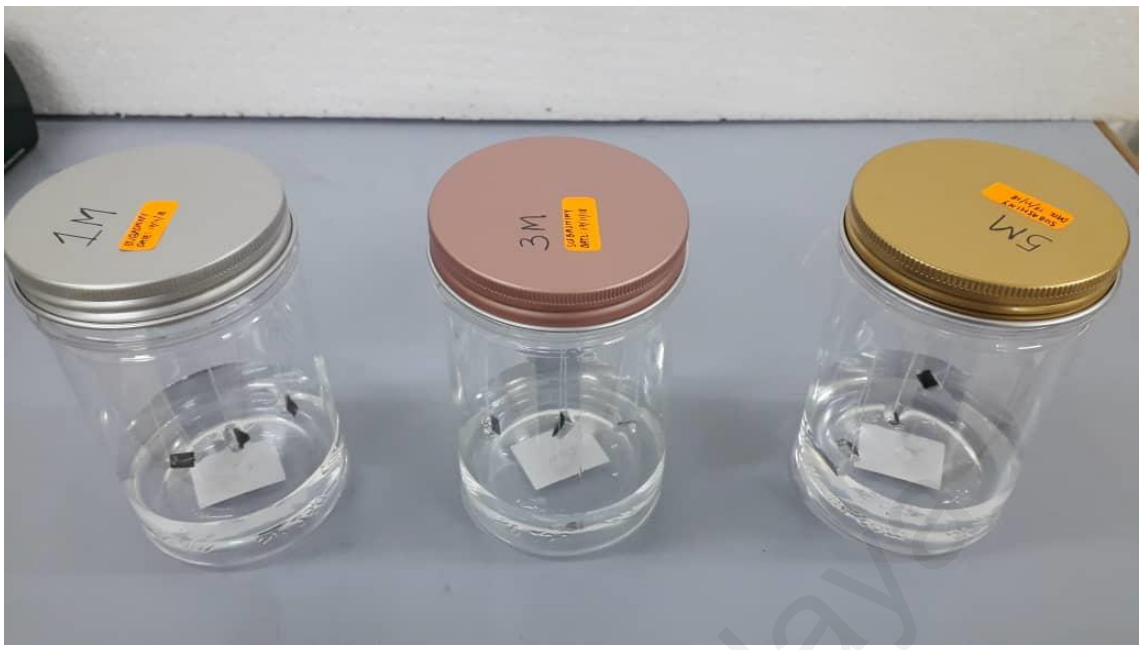

Figure 3.4: Immersing the test samples in NaCl solutions of 1M, 3M and 5M

2) Post the 20h mark, the electrodes were washed using distilled water and dried with tissue paper.
3) The total exposed surface area of the working electrode was 1.1304 cm^2.

The same was repeated on Al-10% GNP and Al-15% GNP samples.

- Conducting Electrochemical Test

1) To obtain the CPP curves, the potential was scanned in the forward direction from -0.1 to 0.5 mV against Pt at a scan rate of 3.0mV/s, followed by the reversal of the potential in the backward direction.
2) The corrosion current, corrosion potential, anodic slope, and cathodic slope values were obtained from the extrapolation of anodic and cathodic Tafel lines located next to the linearized current regions.
3) The electrochemical measurements were conducted after an immersion period of 20h for the three-cell electrode configuration in the test solution.

All measurements were also carried out at room temperature in freely aerated solutions.

3.2.2 Surface Characterization

1) The SEM and EDS investigation were conducted on the working surface of the Al/GNP samples after their immersion in 1 M, 3M and 5M NaCl solutions for 20 hours.
2) The SEM images were carried out by using a Phenom ProX scanning electron microscope with element identifier using the Energy Dispersive Spectrometer attached to identify the post-corrosion surface morphology to compare how immersion in NaOH solution of different degree of concentration affects a Al/GNP sample with different composition of corrosion-inhibiting purposed graphene nanoplatelets.

CHAPTER 4: RESULTS AND DISCUSSION

4.1 Fabrication of Al/GNP composites

Previous research has shown that the direct mixing of carbon powder, in micro and even nano sizes, into molten aluminum is impractical due to the extremely poor carbon wettability of liquid aluminum (Baumli, 2010). This results in highly porous and non-homogeneous composites. However, it is possible to resolve this issue by adding molten alkali chloride and sometimes fluoride to the mixture. Compared with this method, however, the manufacture of aluminum-graphene nanocomposite composites using powder metallurgy technique is much less challenging and easy to do with equipment readily available in the institution.

Powder metallurgy is defined as the compression of various metal powders into finished and semi-finished components (EPMA, n.d.). After compression material is subjected to heating in a furnace under a progressive atmosphere at a high temperature in order to obtain a satisfactory strength, density without losing essential shape. The powder metallurgy technique involves four main steps: the powder fabrication, powder mixture, powder compaction and powder sintering. Aluminum and graphene are the matrix material and the reinforcing material, respectively, used in this powder metallurgy process.

The Al / GNP powders were prepared by mechanical mixing process. The process parameters were based on literature (Jagadish, 2014) (Ramesh, 2014) (Swamy, 2016). The mechanical mixing process produced a uniform mixture of aluminum and GNP powder. Al powder was placed in ball milling set up consist of steel balls 10 mm diameter. The mixing process is continued for a duration of 2 hours at 200 rpm to achieve uniform mixing for different compositions of Al / GNP materials. This is followed by compaction process, by which the metal powders are pressed into compacts of craved shape with

satisfactory quality in order to withstand the discharge from the devices and ensuing taking care of up to culmination of sintering with no breaking. The powder compaction process was carried out with using Universal Testing Machine (UTM) under a load of 80 - 85 kN in the die. The compacted specimens of Al / Graphene were 15 mm in diameter. The working surface after pressing is called compacted green specimen, as shown above Figure 3.1.

Sintering can be characterized as the warming of a free or compacted total of metal powders under the dissolving purpose of base metal with or without the use of external weight, so that entomb particulate holding converts into thicker material (EPMA, n.d.). It could therefore be regarded as a dynamic move without liquefying from the condition of metallic particles to a huge state which should be free of porosity and have physical and mechanical properties. Sintering results in solid holding between quality particles, densification and dimensional control. The compacted specimens are placed in the muffle furnace and heated at a recrystallization temperature of 600oC for approximately 6h, after which they have been cooled. Based on literature, this temperature was chosen as the sintering temperature of aluminium and its typical alloys is in the range of 590-620^{o}C (AZoM, 2002).

4.2 Optical microscopy (OM)

After grinding and polishing the three different types of sintered and compacted Al/GNP, the mirror-finished surface was viewed under optical microscope. The following Figures 4.2, 4.3 and 4.4 show the difference in grain size Al-5% GNP, Al-10% GNP and Al-15% GNP under a magnification of 200 microns.

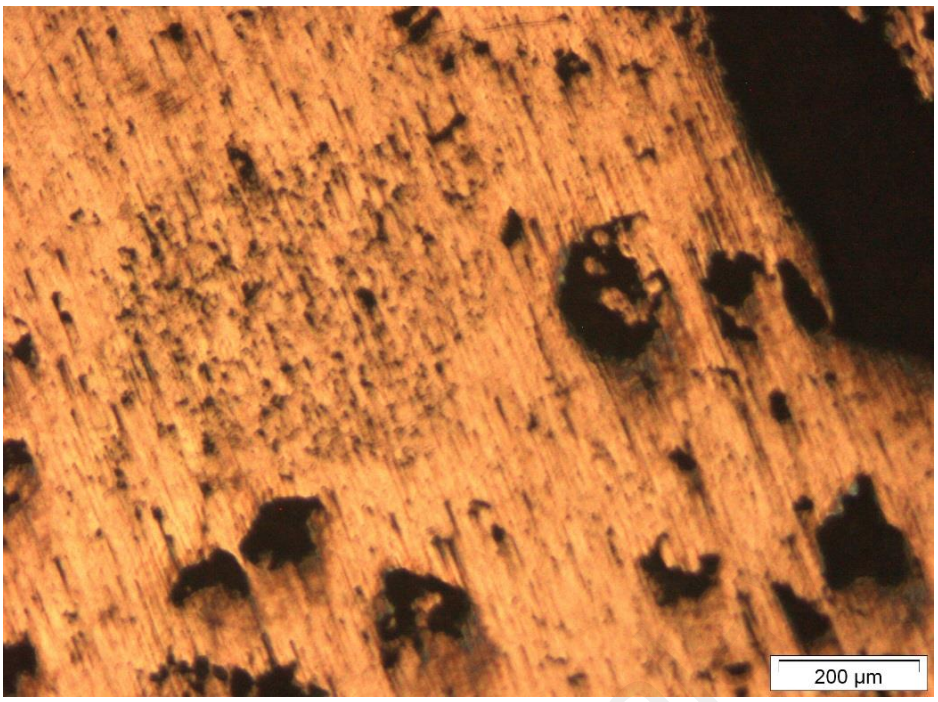

Figure 4.1: Optical micrographs of sintered and compacted Al-5% GNP composite

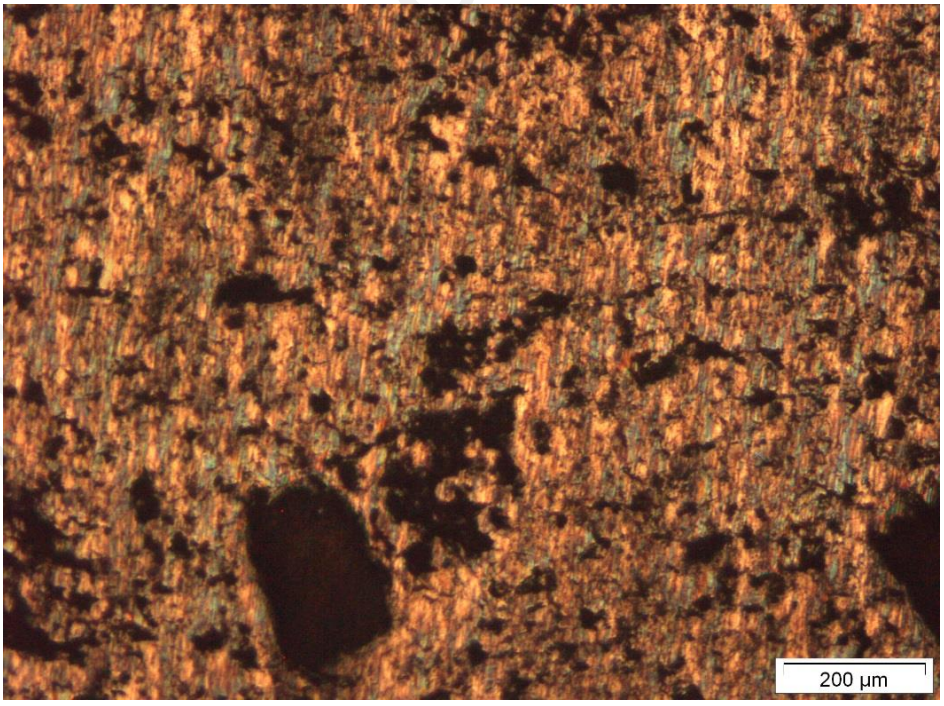

Figure 4.2: Optical micrographs of sintered and compacted Al-10% GNP composite

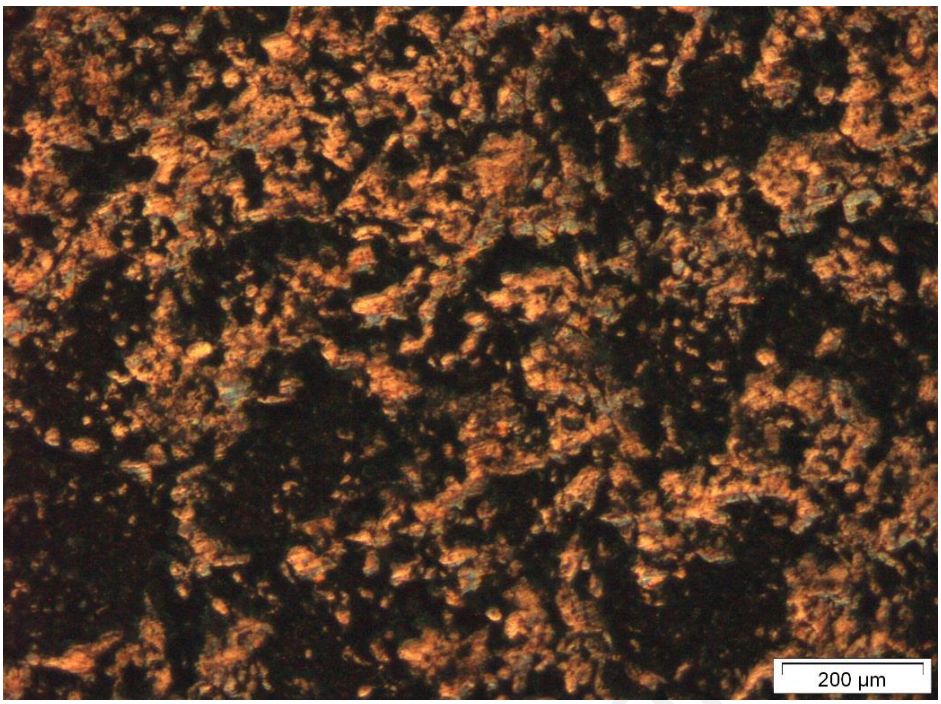

Figure 4.3: Optical micrographs of sintered and compacted Al-15% GNP composite

Figure 4.2 shows the composite with Al-5% GNP composition exhibiting a surface with the smallest pore structures compared to the other two composites. This is inferred from the surface that looks smoother but with not much visible pores. Figure 4.3 shows the composite with Al-10%GNP composition exhibiting a surface with pore structures larger than the Al-10%GNP variant but comparatively smaller than the Al-15%GNP variant. Figure 4.4 shows the composite with Al-15%GNP composition exhibiting a surface with the largest pore structures than the Al-5%GNP and Al-10%GNP variants.

The Al-15%GNP's graphene presence in Figure 4.4 is more obvious compared to Figure 4.2 and 4.3 due to the high concentration of graphene distributed in the composite

4.3 Electrochemical test

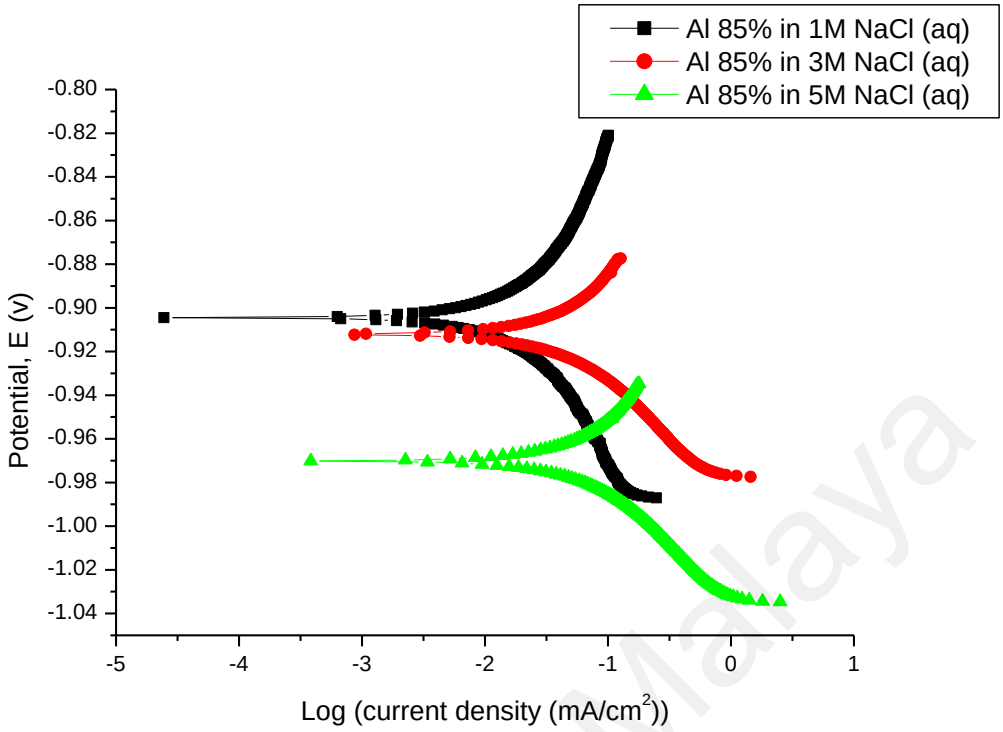

Figure 4.4: Potentiodynamic Polarization Curve for Al-15% GNP

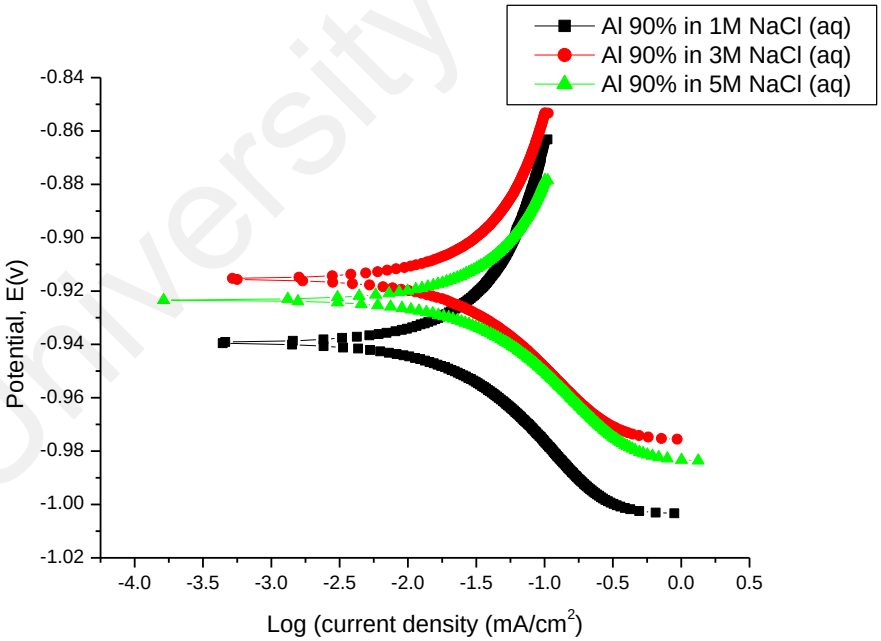

Figure 4.5: Potentiodynamic Polarization Curve for Al-10% GNP

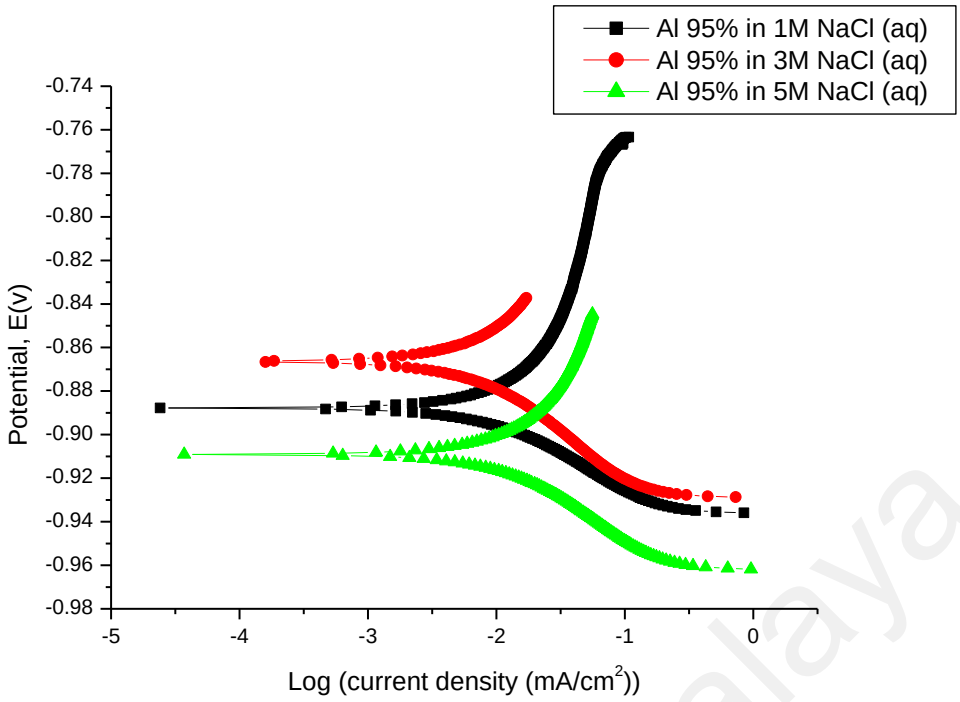

Figure 4.6: Potentiodynamic Polarization Curve for Al-5% GNP

Table 4.1: Corrosion parameters obtained from Potentiodynamic Polarization Curves shown in Fig. 16, 17, and 18 for the different Al electrodes

Test Material	Parameters					
	β_c / mV dec^{-1}	E_{Corr} / mV	I_{Corr}/ µA cm^{-2}	β_a / mV dec^{-1}	B	R_p
Corrosion medium NaCl (aq) 1M						
Al-5%GNP	10.2	-904.451	1.567	10.5	2.249527	1.435563
Al-10%GNP	10.5	-935.513	3.270	10.8	2.314758	0.707877
Al-15%GNP	10.5	-904.284	4.111	10.1	2.238286	0.544463
Corrosion medium NaCl (aq) 3M						
Al-5%GNP	10.0	-864.966	1.109	11.0	2.277433	2.053591
Al-10%GNP	10.4	-905.854	3.680	10.6	2.282402	0.620218
Al-15%GNP	10.2	-928.127	6.388	10.1	2.206468	0.345408
Corrosion medium NaCl (aq) 5M						
Al-5%GNP	10.5	-893.893	1.991	10.2	2.249527	1.129848
Al-10%GNP	10.5	-934.060	4.385	10.2	2.249527	0.513005
Al-15%GNP	10.3	-969.939	9.542	10.4	2.249947	0.235794

Corrosion takes place in various forms in all kinds of materials, depending on the definition. It is most note-worthy to take place in metallic elements. So, in an aluminium-graphene nanocomposite, the corrosion attacks the metallic elements of the MMC. The aluminum corrosion mechanism is caused by the anodic oxidation of the working electrode and the cathode reduction process. This reduction process uses electrons released during aluminum oxidation. The anodic and cathodic reaction that occur on the respective electrodes are given below (E. Sherif, 2006)

At cathode:

$O_2 + 2H_2O + 2e^- \rightarrow 2OH + 2OH^-$

$OH + e^- \rightarrow OH^-$

At anode:

$Al + 3OH^- \rightarrow Al(OH)_3 + 3e^-$

$2Al(OH)_3 \rightarrow Al_2O \cdot 3H_2O$

At the cathode of the electrochemical cell, reduction process of oxygen takes place using electrons released at the anode. As a result, hydroxide ions are formed in the electrolyte medium. On the other hand, the anodic oxidation process generates Al^{3+} which will then merge with these hydroxide ions and become aluminium hydroxide. Upon further oxidation, this becomes aluminium oxide (E. Sherif, 2006). These reactions happen simultaneously. So, it is possible to slow down or stop the corrosion process from expanding further if any external factor which restricts either the anodic oxidization or prevents the contact of OH^- ions is introduced.

Cyclic potentiodynamic polarization (CPP) test was chosen as the electrochemical test to study the corrosion behaviour of the Al-5%GNP, Al-10%GNP and Al-15%GNP Al-GNP composites in NaCl solutions of 1M, 3M and 5M. CPP test is one of the most often technique to determine the vulnerability of a metal matrix to pitting corrosion. When the potential is swept in a single cycle or less, hysteresis can be found forming and recorded in the CPP curves. Size of the hysteresis is examined together with the differences between the values of the open circuit corrosion potential and the passivation potential. Typically, presence of hysteresis on these curves indicate presence of pitting, while the size of the loop is relates to the amount of pitting. It involves changing the potential of the working electrode and monitoring the current which is produced as a function of time or potential.

In this experiment, CPP was carried out after immersing each type of test material in an alkaline corrosive environment of 1M, 3M and 5M for 20 hours. The anodic and cathodic polarization curves recorded for the Al-5%GNP, Al-10%GNP, Al-15%GNP Al-GNP composites in 1M, 3M and 5M NaCl solution are shown in Figure 4.4, 4.5 and 4.6. The measured i_{corr}, E_{corr}, B_a and B_c values are summarized in Table 4.1.

The I_{corr} value, the current between the local anodes and cathodes, of Al-5%GNP in NaCl 1M is 1.567 µA, in NaCl 3M slightly higher at 1.109 µA and even more higher at 1.991 µA in NaCl 1M. For Al-10%GNP in NaCl 1M, the I_{Corr} value is 3.270 µA while it increased to 4.305 µA being tested in NaCl 5M solution. For Al-15%GNP sample, I_{Corr} value increased the same as the former, being at 4.111 µA in NaCl 1M solution and at 9.542 µA in NaCl 5M solution. When compared between Al-5%GNP and Al-15%GNP in NaCl 1M solution, the latter's I_{Corr} value is higher, as in the other two corrosive liquid molarity.

It is to be noted that corrosion current density (I_{corr}) values impart that the higher I_{corr} value indicates that metal possesses less corrosion resistance under the polarization status and lower values show better corrosion resistance (Shrivastava S., 2004). So, it is correct that the I_{Corr} value of the test materials where seen smaller in NaCl 1M solution, compared to 5M as the composite interface has better corrosion resistance to a corrosive solution of lesser concentration.

However, after getting dispersed with more GNP, the Al/GNP composite is showing lesser corrosion resistance to solutions of the same molarity. The higher corrosion rate of Al/GNP composite of Al-15%GNP composition than Al-5%GNP is possibly due to the agglomeration of the graphene nanoplatelets particles in the metal matrix and them being more cathodic relative to the matrix. In the presence of an electrolyte, this leads to galvanic corrosion. The presence of GNP and the increase of its content seem to further induce the anodic dissolution of aluminium in the chloride solution, thus the higher I_{Corr} value of Al-15%GNP in all the different solution molarities, compared to Al/GNP composite with lesser GNP presence. Aluminium undergoes galvanic corrosion of Al can occur when it comes in contact with a more noble metal or other electron conductor, which has a higher chemical potential than aluminium (Kautek, 1988). Even a very small concentration of impurities on the metal surface could greatly aggravate its galvanic corrosion by serving as an electrode for the process of oxygen reduction (Zhou F, 2013).

The polarization resistance, R_p, was calculated for Al-5%GNP, Al-10%GNP and Al-15%GNP with CPP conducted in each of the 1 M, 3 M and 5 M NaCl solutions using Tafel plot with Stern-Geary expression. The Stern-Geary equation (Zhou F, 2013) is provided below for the evaluation of R_p,

$$R_p = \frac{B}{i_{corr}}$$

Where

$$B = \frac{b_a b_c}{2.3(b_a + b_c)}$$

b_a = anodic slope, b_c = cathodic slope and I_{Corr} = corrosion current density.

The b_a, b_c, I_{corr} and their corresponding polarization resistance values obtained are tabulated in Table 4.1. Based on this result and the CPP curves, when more GNP was added to Al/GNP composite, the anodic slope increases while the cathodic slope decreases.

This phenomenon is attributed to the amount of GNP presence in the MMC, which act as a barrier that resists the corrosion of the aluminium metal at the anode (working electrode). From Table 4.1, it can be seen that R_p of Al-5%GNP in 1M solution is higher than in 5M solution and compared to Al-15%GNP. These data further supports the earlier discussion made, specifying how graphene presence weakens polarization resistance, especially in increasingly corrosive environment.

Besides the occurrence of galvanic corrosion, the phenomenon of pitting corrosion could also be observed in these test samples. This type of corrosion, which is typically associated with the Al matrix, can also be determined from the anodic polarization measurement. When exposed to the environment, all kinds of Al component immediately forms Al_2O_3 barrier film. This barrier is the natural protection for the underlying metal from further corrosion. However, upon reaching a critical potential, in the higher anodic region, this oxide layer breaks and the electrolyte may get a way to seep into the matrix of Al. From this, the metal starts to decompose into a soluble complex of aluminium chloride. At this critical potential value, which is also called the pitting potential (E_{pit}),

pitting nucleation starts (Kautek, 1988). The mechanism of pitting corrosion in aluminium is as follows,

$Al = Al^{3+} + 3e^-$

$Al^{3+} + 4Cl^- = AlCl_4^-$

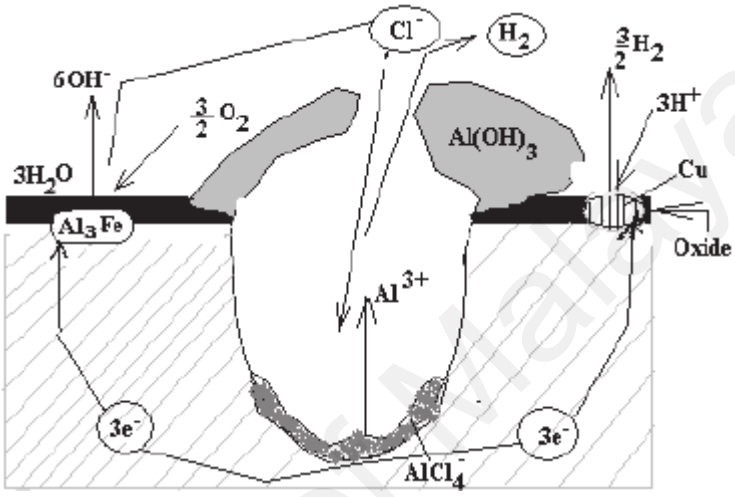

Figure 4.7: Schematic diagram depicting mechanism of Al's pitting process (Mutombo, 2011)

The above described changes are visualized clearly for Al-5%GNP samples immersed in all three types of NaCl molarity, whereas this occurrence is shown to decrease with increasing presence of GNP in the composites. Presence of the biggest hysteresis loop in Al-5%GNP's CPP curve in Figure 4.8 denotes this phenomenon. It has to be noted that earlier the non-mirror finished surfaces of the Al/GNP test coupons were covered with Al foil. This cover-up method is later realized to be not the most ideal, however, due to the unavailability of fresh, new pieces of test coupons, CPP test results obtained using them were still used to evaluate corrosion behavior of Al/GNP composites. It is thought that aluminium from the foil could have influenced the corrosion behavior of the test coupons. In 1M, 3M and 5M NaCl solutions, higher general corrosion attack was recorded in Al-15%GNP, however highest pitting corrosion, evaluated via hysteresis loop size was observed in Al-5%GNP. This contradicting corrosion behavior in hysteresis loop size is

seemed to have been influenced by the presence of aluminium in the form of foil during CPP test. Thus, the pitting corrosion behavior recorded the highest for Al-5%GP may not be accurate.

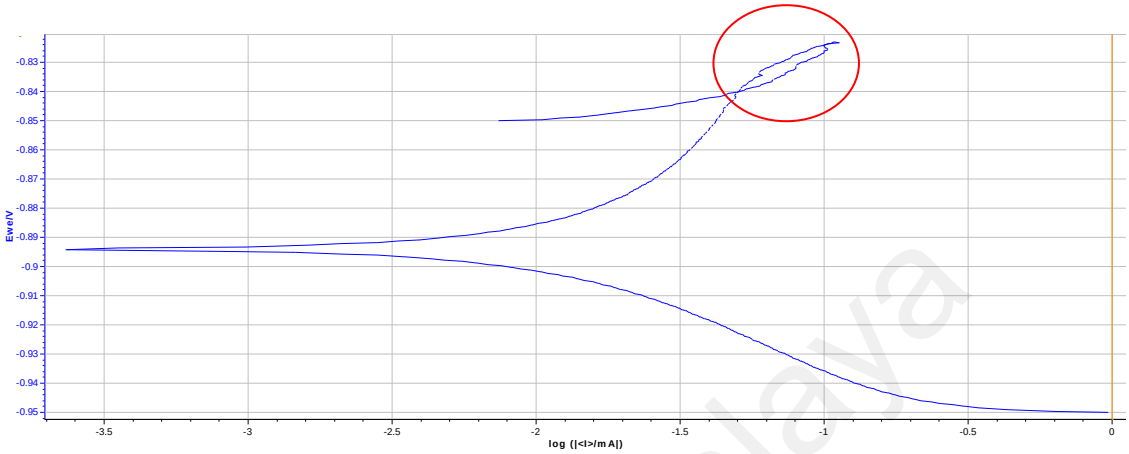

Figure 4.8: Al-5%GNP in 5M solution

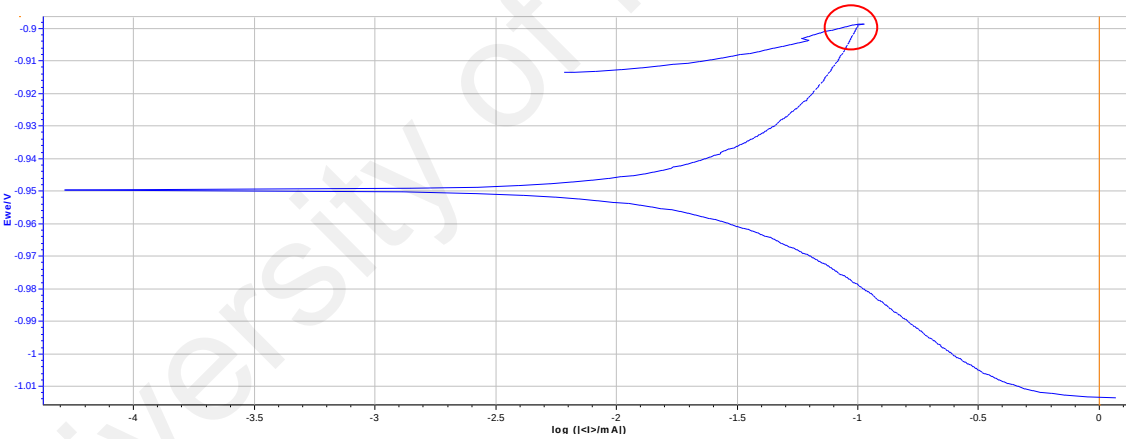

Figure 4.9: Al-10%GNP in 5M solution

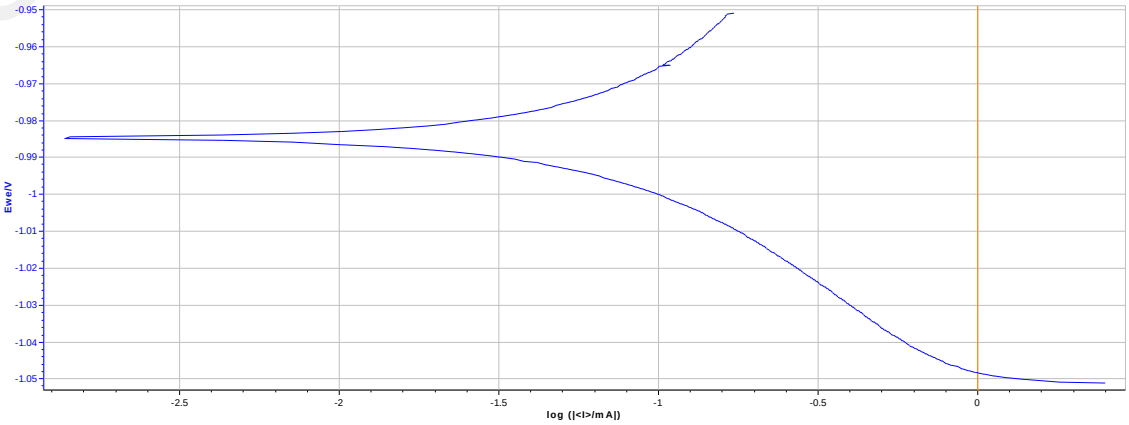

Figure 4.10: Al-15%GNP in 5M solution

4.4 Scanning Electron Microscopy / Energy Dispersive Spectroscopy

The surface morphology of the Al-5%GNP and Al-10%GNP have been observed by taking scanning electron microscopy (SEM) images after the potentiodynamic polarization measurements. The images are shown in Figures 4.11, 4.12, 4.13 and 4.14. Al-15%GNP had degraded to its initial powder form, following the destructive CPP test, so its surface morphology post corrosion test couldn't be identified.

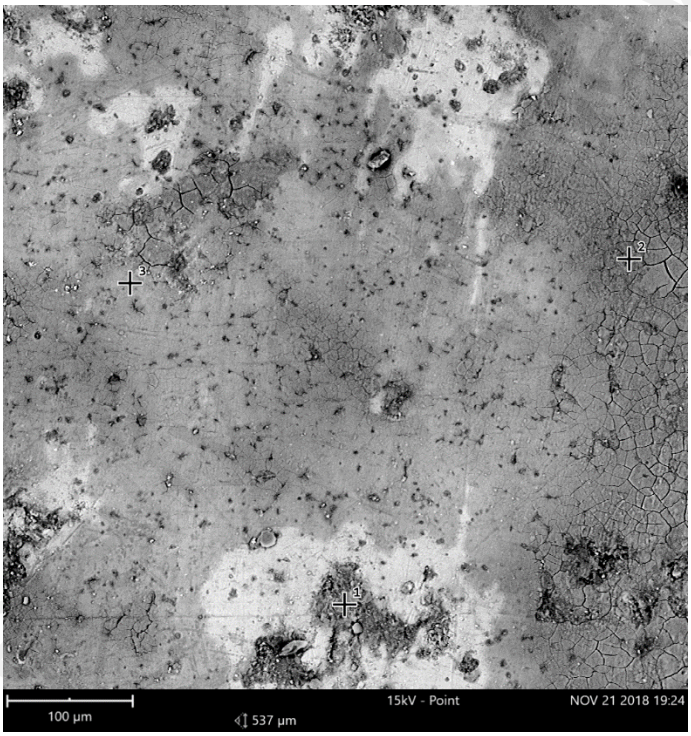

Figure 4.11: Corrosion attacked surface of Al-5%GNP in 1M NaCl

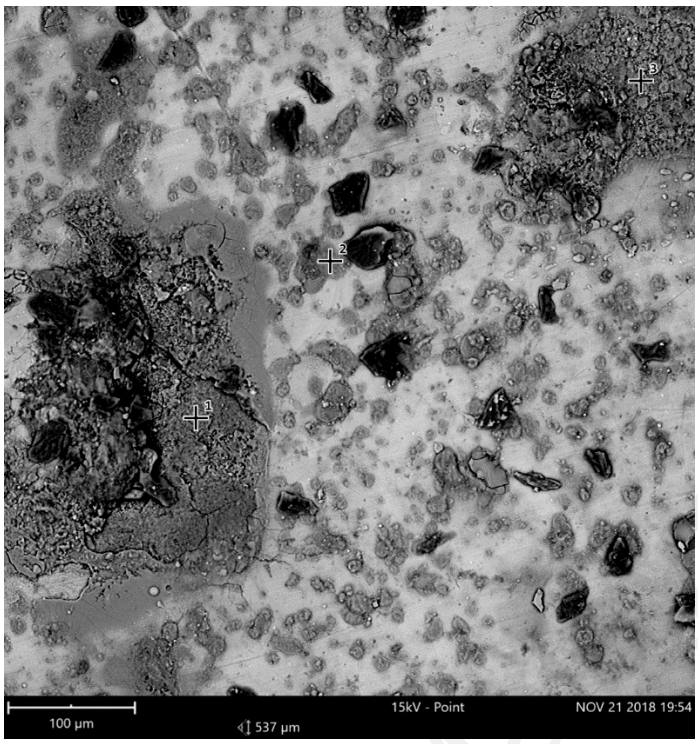

Figure 4.12: Corrosion attacked surface of Al-10%GNP in 1M NaCl

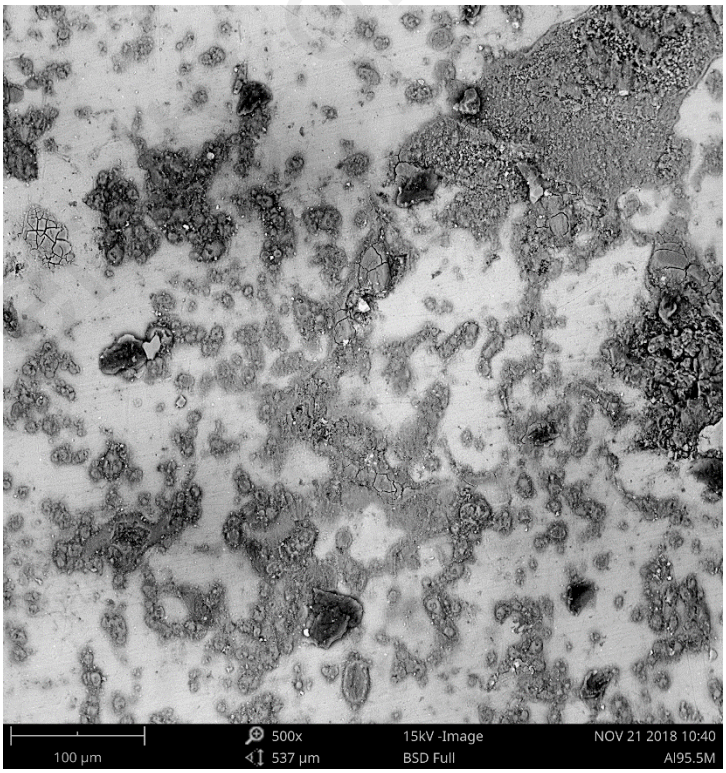

Figure 4.13: Corrosion attacked surface of Al-5%GNP in 5M NaCl

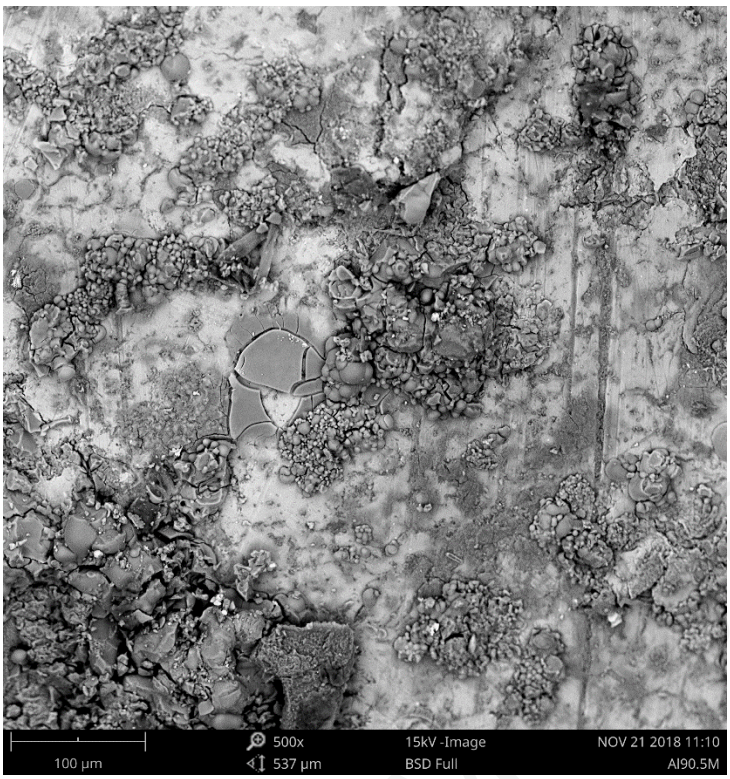

Figure 4.14: Corrosion attacked surface of Al-10%GNP in 5M NaCl

After performing corrosion test, the Al-10%GNP in NaCl 1M, 3M and 5M showed more overall galvanic corrosion all over the surface, compared to Al-5%GNP in similar NaCl 1M, 3M and 5M, indicating substantial corrosion. Pit corrosion was also seen strewn around the surface of Al-5%GNP more than on surface of Al-10%GNP, as indicated by the hysteresis loop of CPP curves.

To further investigate the corrosion mechanism and corrosion products, EDS mapping studies have been performed. For this study, unfortunately, the Al-15% GNP sample could not be used. Post the CPP test, which is destructive in nature, this sample expanded when left untouched for a few days while waiting to conduct the SEM/EDS. Even though each samples were thoroughly cleaned using distilled water and immediately dried to lessen the any after-effects caused by NaCl particles sedimented on the test materials, the reason for this phenomenon could not be accurately identified. So, only Al-5%GNP and Al-10%GNP samples were seen under an SEM.

After subjected to corrosion test, an extremely pitted point (P2) and a mildly corroded (pit) point (P3) are mapped by EDS on a Al-5%GNP tested in 5M NaCl solution, as shown in Figure 4.15, to study the constituents present at the site of corrosion.

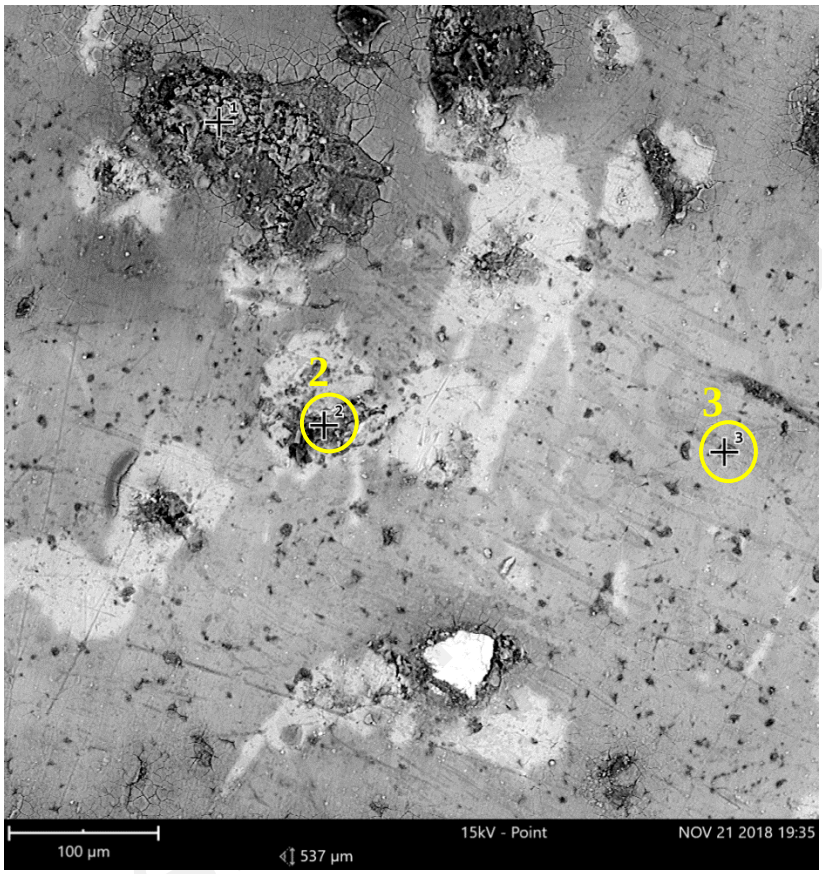

Figure 4.15: SEM image for Al-5% tested in NaCl 5M solution and Point (No.2) and (No.3) highlighted on the surface

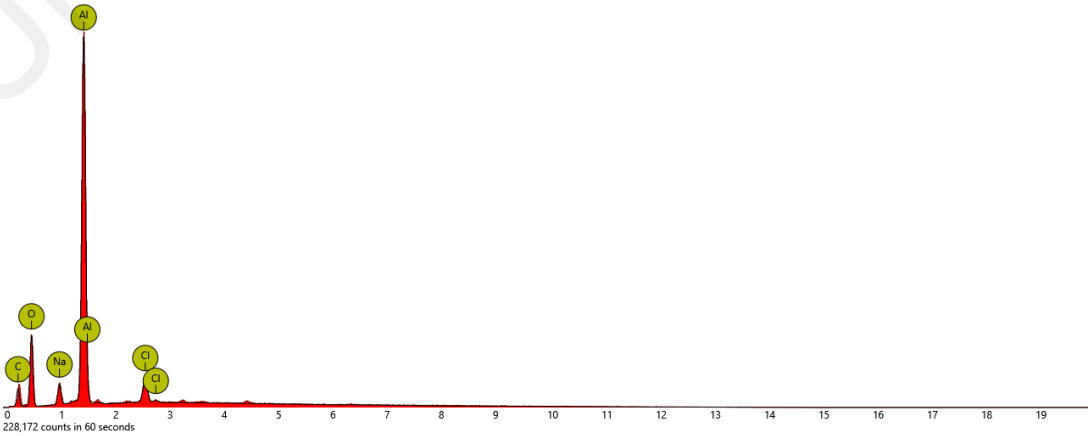

Figure 4.16: EDS chart for Point 2 on surface of Al-5%GNP tested in 5M NaCl

Table 4.2: List of elements present at Point 2 on surface of Al-5%GNP tested in 5M NaCl

Element Number	Element Symbol	Element Name	Atomic Conc.	Weight Conc.
6	C	Carbon	37.09	25.06
8	O	Oxygen	34.01	30.61
13	Al	Aluminium	24.67	37.45
11	Na	Sodium	2.21	2.86
17	Cl	Chlorine	2.01	4.01

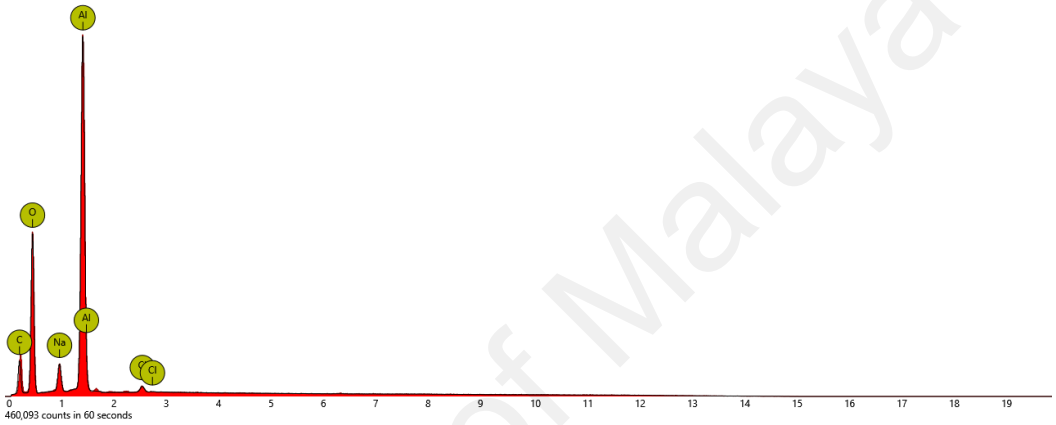

Figure 4.17: EDS chart for Point 3 on surface of Al-5%GNP tested in 5M NaCl

Table 4.3: List of elements present at Point 3 on surface of Al-5%GNP tested in 5M NaCl

Element Number	Element Symbol	Element Name	Atomic Conc.	Weight Conc.
8	O	Oxygen	44.47	42.51
6	C	Carbon	35.36	25.38
13	Al	Aluminium	17.56	28.30
11	Na	Sodium	2.30	3.16

The EDS mapping images, Figure 4.16 and 4.17, of Al-5%GNP were obtained after immersing in 5M NaCl solution and conducting the CPP test. The site of voids were analyzed, and their corresponding EDS spectra are shown in these images. From Fig. 4.16, it is evident that the oxygen atoms are present more on the lesser corroded surface indicating the formation of oxide layer, aluminium's natural way of protecting its surface from the harsh environment. Figure 4.15 shows the SEM image of the corroded area in

the vicinity of voids displaying the regions the graphene had given away. Further, EDS mapping of the corroded specimens ensured that the corroded region exposes the Al, C, and O atoms at the voids.

It is to be noted that previous studies (Etter, 2007) (Muradymov, 2016) have indicated the formation of aluminium carbide (Al_4C_3) due to carbon dissolution at high temperature during the fabrication process. Even small Al_4C_3 presence damages Al/GNP composite materials in aggressive environments, and even in atmospheric conditions. The tablets fabricated for this study were not initially tested for the presence of Al_4C_3. Furthermore, in the post-corrosion study, EDS study performed was sufficient to validate the possible presence of Al_4C_3. Therefore, it is highly possible that Al_4C_3 could have been present in each test sample since the start and this may have contributed to the further deterioration of the Al/GNP composites in corrosive environments.

The mechanical properties of Al/GNP composites made by dispersing the GNP in the metal matrix itself has been reported to have a significant improvement compared to pure aluminium and its alloys (Alam S.N., 2016) (Dasari B.L., 2018) (Kumar P., 2014). Al/GNP composite show an increase in relative density with the addition of graphene in the matrix. However, the addition of GNP beyond 3wt% in the Al matrix leads to a considerable decrease in the relative density of the Al/GNP composites suggesting poor densification. This is possibly due to the formation of a large amount of Al_4C_3 at the interface of the GNP and the Al particles as well as the agglomeration of GNP. Al_4C_3 adversely affects both the sinterability and the densification of the Al/GNP composites. A similar trend is also seen for the hardness of the composites. The hardness of the Al/GNP composites increase up to the addition of 1wt% of GNP. However, the addition of GNP beyond 3 wt% was reported to lead to a large decrease in the hardness of the Al/GNP composites (Alam S.N., 2016). The hardness of the composites possibly reduces

due to the agglomeration of GNP in the Al matrix which also leads to poor densification of the composites. An increase of 28.64% in micro hardness was observed with 0.2 wt% of graphene reinforcement (Dasari B.L., 2018). The tensile strength of the Al/GNP composites continuously decreases with the addition of GNP. This is due to the detrimental effect of Al_4C_3 at the interface of the GNP and the Al matrix. The increase in the wt% of GNP in the Al/GNP composites results in the formation of a higher amount of Al_4C_3 at the interface of the Al matrix and the GNP. So, based on these data, it can be concluded that the even though graphene addition can enhance the mechanical properties of Al/GNP composites, this has to be done in a controlled amount as the increase of GNP above 3% in volume results in a reduction of overall mechanical properties. Not just mechanical properties, gradual increase in GNP, as experimented in the current study, also shows increasing corrosion attack in the Al/GNP composite.

In a nutshell, the increasing addition of GNPs into aluminium matrices seem to have increased the corrosion currents, in this study. This could be attributed to the dislocation densities at the interface of composites, which create crevice attacks (Esmailzadeh, 2018). Al/GNP composite with more GNP presence recorded higher corrosion rate compared to matrices with lesser GNPs. Furthermore, high corrosion attack of Al/GNP composites with higher GNP composition is also inferred to be due to the selective dissolution of aluminium. It has been noted that the dissolution of aluminium is influenced by the force of galvanic corrosion, where graphene nanoplatelets acts as the cathode due to it's nobler than aluminium, which has very active potential.

Immersing the Al-5%GNP in 5M NaCl seemed to have definitely increased the corrosion and this value hasn't been much distinguished for the Al-15%GNP material. The surface morphology of corroded samples, for all three test samples, revealed a lot of cracks and pitting sites. The addition of GNP, as mentioned above, had induced galvanic

corrosion in increasing amount with the utilization of more GNP in the three test samples. This corrosion is highly responsible for propagating the cracks further and resulting in many areas with the top few layers corroded away on the material surface, thus the finding of increasingly corroded test material exposed surface with more utilization of GNP. This has been even been validated by the electrochemical results.

The increasingly corrosive environment further encourages the test materials to form more protective barrier on the surface, as indicated by the higher presence of oxygen on surface of Al-5% GNP and Al-10% GNP in 5M NaCl solution, compared to 1M or 3M NaCl solutions. The presence of these additional oxide components on the surface appeared instrumental in controlling the amount of damage galvanic corrosion was having. However, this may not necessarily be the case for pitting corrosion as more tests need to be conducted to validate the complete efficiency of the oxide layer forming when the Al is placed in a highly harsh and corrosive environment.

It has been previously reported in previous studies (Potts, 2011) (E. Sherif, 2006) that the addition of graphene more than 3% actually influences the reduction of mechanical strength and hardness of Al/G composites. As such, based on current study, addition of more GNP among the three test materials in each NaCl concentration seemingly increase the occurrence of corrosion attack. However, it is not to be denied that addition of GNP of certain amount actually enhances the mechanical properties of Al/G composites in some studies (Dasari B.L., 2018).

.

CHAPTER 5: CONCLUSIONS

This study has been based on the different amount of GNP addition on aluminium matrix and its corrosion behavior in different molarity of corrosive solutions. It was found that Al/GNP with increasing GNP content experienced higher corrosion attack than the others, even though pitting corrosion results prove otherwise. However, this has been earlier explained that certain errors in the methodology could have influenced it. Results obtained from this study suggest that the GNPs acted as effective cathodes to accelerate the corrosion.

From these results, it can be concluded that increasing amount of GNP in a MMC, above a certain limit, actually accelerates rate of corrosion attack experienced by the MMC. It is learnt from this study and previous studies (Kumar P., 2014) (Kirkland, 2012) that more care should be taken while choosing the amount of graphene to be added in the MMC.

Moreover, it is also hoped that different variations of electrochemical tests such as electrical impedance spectrocopy (EIS) and chronoamperometry are used to validate if it is indeed that increasing GNP addition in the metal matrix makes the composite more susceptible to corrosion attack, especially galvanic corrosion.

Furthermore, more studies need to be conducted on how Al/GNP composites fabricated with GNP coated on the surface fare in similar increasingly corrosive environment and if properties of GNP coatings vs matrix dispersion are comparable. It is largely unknown whether the natural corrosion protection behavior of Al, by forming oxide barrier, is the same when graphene is instead coated on the test material surface, especially when the alkalinity or acidity of environment is increased.

REFERENCES

Alam S.N., K. L. (2016). Mechanical properties of aluminium based metal matrix composites reinforced with graphite nanoplatelets. *Materials Science & Engineering A*, 16-32.

Aneja, K. e. (2017). Functionalised graphene as a barrier against corrosion. *FlatChem*, 13-19.

AZoM. (14 Nov, 2002). *Powder Metallurgy - Sintering Temperatures for Some Common Metals.* Retrieved from AZO Materials: https://www.azom.com/article.aspx?ArticleID=1727

Baumli, P. e. (2010). Perfect wettability of carbon by liquid aluminum achieved by a multifunctional flux. *J. Material Science*, 5177-5190.

CHAPTER 4 - TYPES OF CORROSION: Materials and Environments. (2006). In A. Z., *Principles of Corrosion Engineering and Corrosion Control* (pp. 120-270). Butterworth-Heinemann.

Dasari B.L., M. M. (2018). Mechanical properties of graphene oxide reinforced aluminium matrix composites. *Composites Part B*, 136–144.

Davis, J. e. (1999). Corrosion of aluminium and aluminium alloys. *ASM International*, 1-43.

E. Sherif, S.-M. P. (2006). Effects of 1, 4-naphthoquinone on aluminum corrosion in 0.50 M sodium chloride solutions. *Electrochim. Acta 51*, 1313-1321.

EPMA. (n.d.). *Powder Metallurgy Process*. Retrieved from European Powder Metallurgy Association: https://www.epma.com/powder-metallurgy-process

Esmailzadeh, S. e. (2018). Interpretation of Cyclic Potentiodynamic Polarization Test Results for Study of Corrosion Behavior of Metals: A Review. *Protection of Metals and Physical Chemistry of Surfaces, 54*(5), 976–989.

Etter, T. e. (2007). Aluminium carbide formation in interpenetrating graphite/aluminium composites. *Materials Science and Engineering: A, 448*(1-2), 1-6.

Frank I.W., T. D. (2007). Mechanical properties of suspended graphene sheets. *Journal of Vacuum Science & Technology B: Microelectronics and Nanometer Structures Processing, Measurement, and Phenomena*.

Geim, A. K. (2007). The rise of graphene. *Nature materials*, 163-191.

Gong, S. e. (2017). Learning from nature: constructing high performance graphene-based nanocomposites. *Materials Today, 20*(4), 210-219.

Jagadish, B. (2014). Characterization of Al based Nano composites Using Powder Metallurgy Technique. *SSRG Int. J. of Mech. Eng., 2*(7), 131-147.

Jang, H. e. (2017). Reduced graphene oxide as a protection layer for Al . *Applied Surface Science*, 1-7.

Katsnelson, M. (2007). Graphene: carbon in two dimensions. *Materials Today, 10*(1-2), 20-27.

Kautek, W. (1988). The galvanic corrosion of steel coatings: aluminium in comparison to cadmium and zinc. *Corosion Science, 28*, 173–99.

Kirkland, N. e. (2012). Exploring graphene as a corrosion protection barrier. *Corrosion Science*, 1-4.

Kumar P., X. M. (2014). Graphene Reinforced Metal Matrix Composite (GRMMC): A Review. *Procedia Engineering* (pp. 1033-1040). Elsevier Ltd.

Lee, D. K. (2012). Different Characterization Techniques to Evaluate Graphene and Its Properties. In P. G. Mukhopadhyay, *Graphite, Graphene, and Their Polymer Nanocomposites.* Florida: CRC Press .

Liu J., J. K. (2013). Mechanical properties of graphene platelet-reinforced alumina ceramic composites. *Ceramics International*, 6215-6221.

Muradymov, R. e. (2016). Enhancement of the mechanical properties of aluminum-graphene composites. *AIP Conference Proceedings.* Boston: American Institute of Physics.

Mutombo, K. e. (2011). Corrosion Fatigue Behaviour of Aluminium 5083-H111 Welded Using Gas Metal Arc Welding Method. In K. e. Mutombo, *Arc Welding.*

Obot, L. e. (2018). Electrochemical frequency modulation (EFM) technique: Theory and recent practical applications in corrosion research. *Journal of Molecular Liquids, 249*(12), 83–96.

Potts, J. e. (2011). Graphene-based polymer nanocomposites. *Polymer*, 5-25.

Ramesh, B. (2014). Characterization of Al Based Nano composites Using Powder Metallurgy Technique. *Int. J. Of Research In Aeronautical & Mech.Eng., 2*(2), 131-147.

Rashad, M. e. (2015). Investigation on microstructural,mechanica land electrochemical properties of aluminum composites reinforced with graphene nanoplatelets. *Progress in Natural Science: Materials International, 25*, 460–470.

Richards, J. (1887). *Aluminium: its history, occurence, properties, metallurgy and applications, including its alloys.* Philadelphia: Henry Carey Baird & CO.

Sahu S.C., S. A. (2013). A facile electrochemical approach for development of highly corrosion protective coatings using graphene nanosheets. *Electrochemistry Communications*, 22-26.

Shaw B.A., K. R. (2006). What is corrosion? *The Electrochemical Society Interface*, pp. 24–26.

Sherif E.M., e. (2011). Effects of Graphite on the Corrosion Behavior of Aluminum-Graphite Composite in Sodium Chloride Solutions. *Int. J. Electrochem. Sci*, 1085-1099.

Shin, S. B. (2015). Deformation behavior of aluminum alloy matrix composites reinforced with few-layer graphene. *Composites: Part A, 78*(35), 42-47.

Shrivastava S., A. I. (2004). Medical Device Materials : Proceedings from the Materials & Processes for Medical Devices Conference 2003, 8-10 September 2003, Anaheim, California. *Materials Park, OH: ASM International.*

Swamy, H. e. (2016). Development And Characterization Of Aluminum -Graphene Metal Matrix Composites Using Powder Metallurgy Route. *International Journal For Technological Research In Engineering, 3*(10), 2648-2652.

Tiburcio, C. e. (2016). Electrochemical Corrosion of Ferritic 409 and 439 Stainless Steels 409 and 439 in NaCl and H2SO4 solutions. *Int. J. Electrochem. Sci., 11*(9), 1080 - 1091.

Tsetseris, L. e. (2014). Graphene: An impermeable or selectively permeable membrane for atomic species? *Carbon*, 58-63.

Um, J. e. (2018). Investigation of the size effect of graphene nanoplatelets (GnPs) on the anti-corrosion performance of polyurethane/GnP composites. *RSC Adv., 8*, 17091–17100.

Watson A.B., Y. J. (2012). A unified formula for light-adapted pupil size. *Journal of Vision*.

Yolshina, L. e. (2016). Novel aluminum-graphene and aluminum-graphite metallic composite materials: Synthesis and properties. *Journal of Alloys and Compounds*, 449-459.

Yu, Z. e. (2015). Fabrication of graphene oxide–alumina hybrids to reinforce the anti-corrosion performance of composite epoxy coating. *Applied Surface Science, 361*(54), 986–996.

Zhang, T. e. (2017). Effects of graphene nanoplates on microstructures and mechanical properties of NSA-TIG welded AZ31 magnesium alloy joints. *Trans. Nonferrous Met. Soc. China, 27*, 1285−1293.

Zheng SX, L. J. (2010). Inorganic–organic sol gel hybrid coatings for corrosion protection. *J. Sol-Gel Sci. Technol.*, 74–187.

Zhou F, L. Z. (2013). Enhanced room temperature corrosion of copper in the presence of graphene. *ACS Nano, 7*(8), 6939–47.